Characterization of 2D Materials : Challenges and Opportunities

Robert M. Wallace

Professor and Erik Jonsson Distinguished Chair

University of Texas at Dallas

rmwallace@utdallas.edu

https://sites.google.com/site/robertmwallace01/

This work was supported in part by:

- The Center for Low Energy Systems Technology (LEAST), one of six centers supported by the STARnet phase of the Focus Center Research Program (FCRP), a Semiconductor Research Corporation (SRC) program sponsored by MARCO and DARPA.
- The SWAN Center, a SRC center sponsored by the Nanoelectronics Research Initiative and NIST.
- The US/Ireland R&D Partnership (UNITE) under the NSF award ECCS-1407765.

Acknowledgements

- Students
  - Angie Azcatl, Hui Zhu, Chris Smyth, Qingxiao Wang, C. Zhang
- Research Scientists
  - Rafik Addou, Xiaoye Qin, Stephen McDonnell (Now @ UVa)
- Colleagues
  - K.J.Cho (DFT of interfaces), Chris Hinkle (MBE), Jiyoung Kim (Raman),
  - Moon Kim (HRTEM), Chad Young (Device Measurements)
- Collaborators
  - Joerg Appenzeller (Purdue), Paul Hurley (UCC/Tyndall), Ali Javey (UC Berkeley), Josh Robinson (Penn State)

DARPA MTO MICROSYSTEMS TECHNOLOGY OFFICE

STARnet

LEAST

Center for Low Energy Systems Technology

NSF

NIST National Institute of Standards and Technology U.S. Department of Commerce

NRI nanoelectronics RESEARCH INITIATIVE

SWAN South West Academy of Nanoelectronics

- Materials Challenges
- Tools and Methods
- TMDs
- Summary

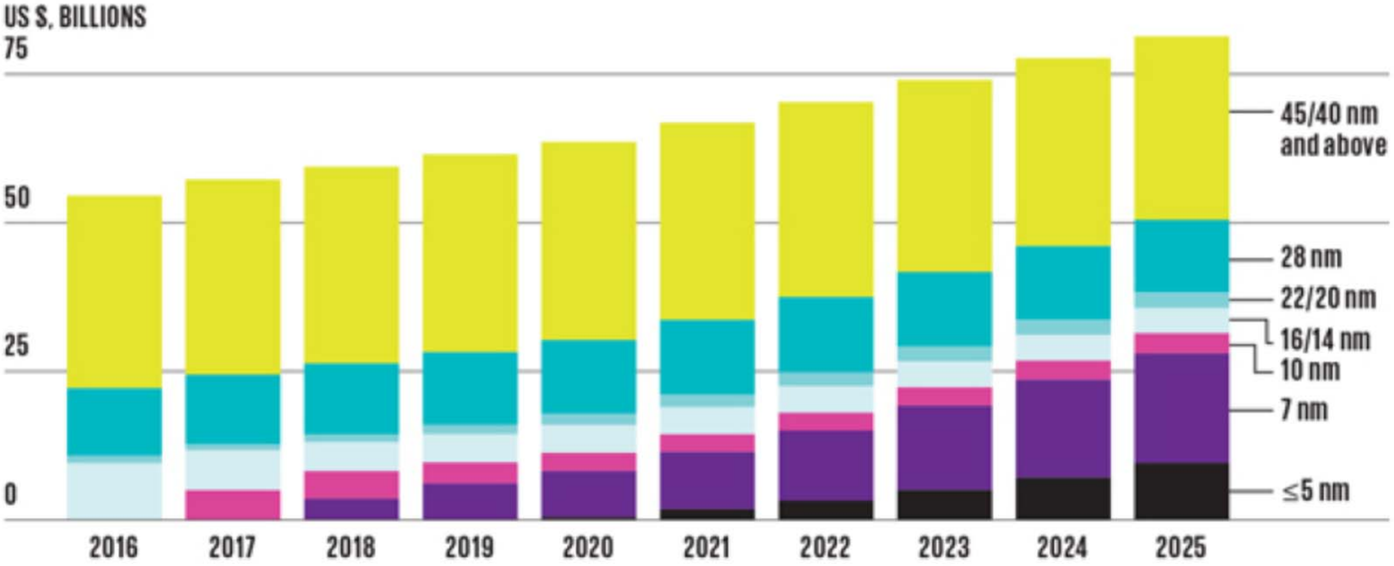

Source: IBS

The Evolving Foundry Market: Chips built with 10-nanometer technology will come first. But International Business Strategies projects that Apple and others will be drawn to the next node in line: 7 nm.

IEEE Spectrum, 30 Dec 2016

UT DALLAS

Rethinking “Classical” Transistor design

- CMOS performance requirements point toward alternative…
  - Materials (e.g., Si→Ge→III-V→2D?)
  - Structures (planar → 3D Fin FET → Gate all around)
  - Devices (MOSFET → TFET)

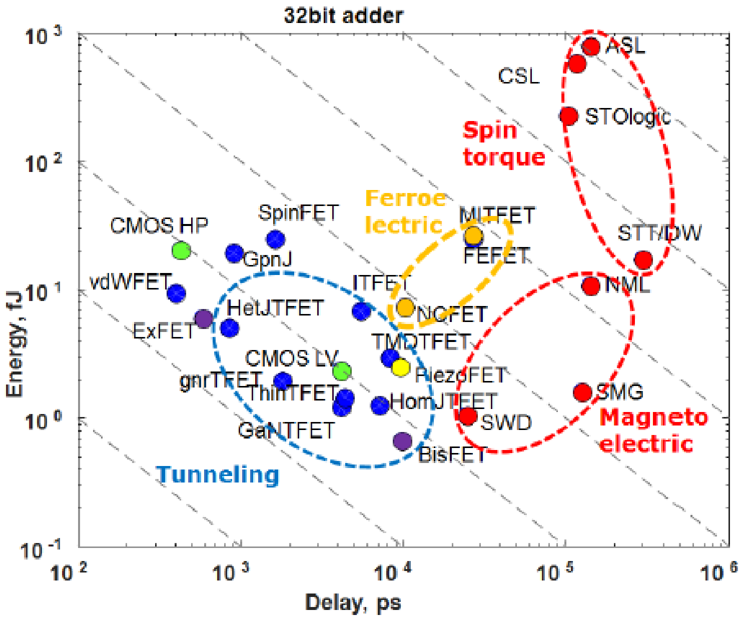

Fig. 5. Switching energy vs. delay of a 32-bit adder.

<u>Beyond CMOS – Some Recent References</u>

Nikinov and Young, JxCDC (2015), Proc. IEEE (2013); Bernstein, et al., Proc. IEEE 98 (2010) 2169; Seabaugh and Zhang, Proc. IEEE 98 (2010) 2095; D. Jena, Proc. IEEE (2013)

2D Materials for Nanoelectronics

Boron Nitride

http://en.wikipedia.org/wiki/Boron_nitride

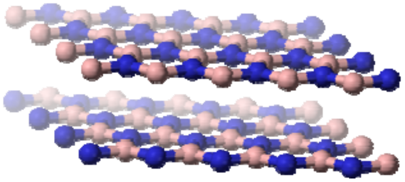

Chhowalla et al. Nature Chemistry 5 (2013) 263

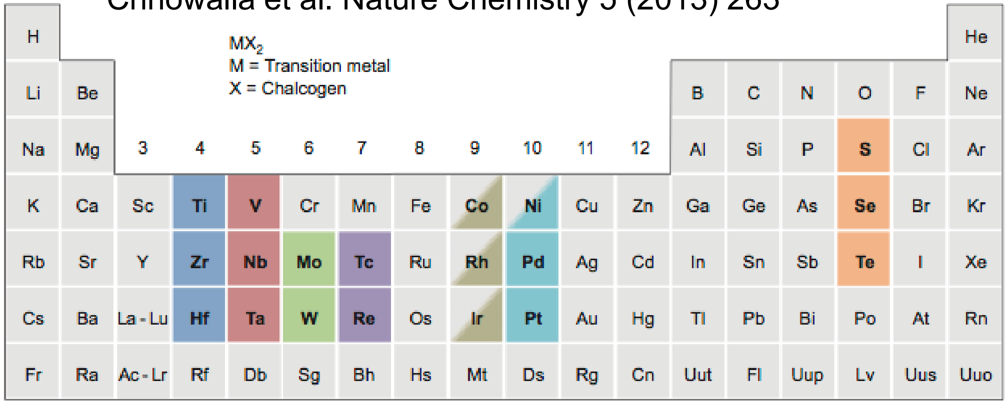

MX_2
M = Transition metal
X = Chalcogen

H																	He
Li	Be											B	C	N	O	F	Ne
Na	Mg	3	4	5	6	7	8	9	10	11	12	Al	Si	P	S	Cl	Ar
K	Ca	Sc	Ti	V	Cr	Mn	Fe	Co	Ni	Cu	Zn	Ga	Ge	As	Se	Br	Kr
Rb	Sr	Y	Zr	Nb	Mo	Tc	Ru	Rh	Pd	Ag	Cd	In	Sn	Sb	Te	I	Xe
Cs	Ba	La - Lu	Hf	Ta	W	Re	Os	Ir	Pt	Au	Hg	Tl	Pb	Bi	Po	At	Rn
Fr	Ra	Ac - Lr	Rf	Db	Sg	Bh	Hs	Mt	Ds	Rg	Cn	Uut	Fl	Uup	Lv	Uus	Uuo

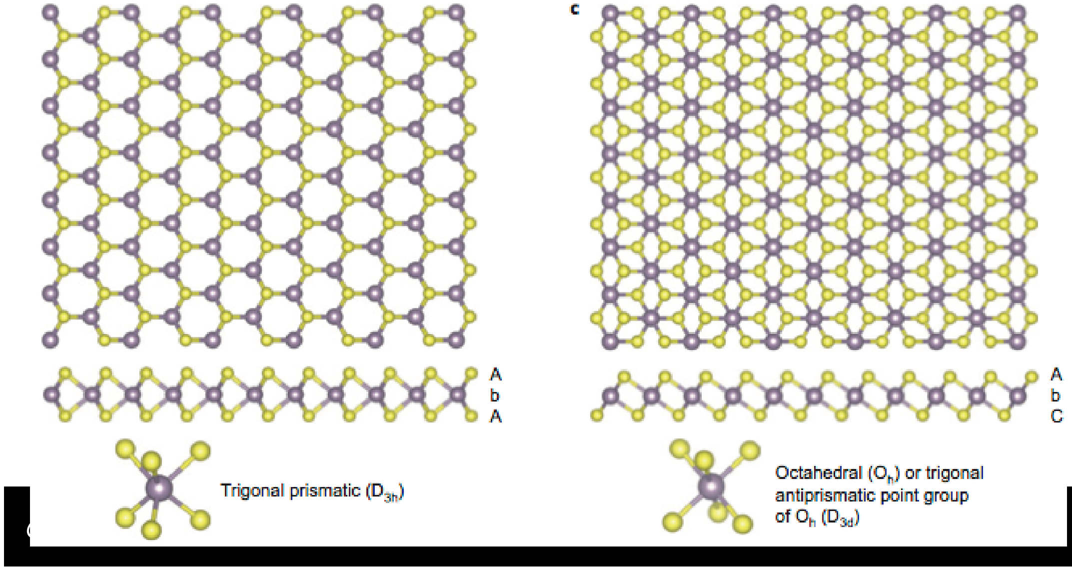

Trigonal prismatic (D_{3h})

Octahedral (O_h) or trigonal antiprismatic point group of O_h (D_{3d})

MoS_2

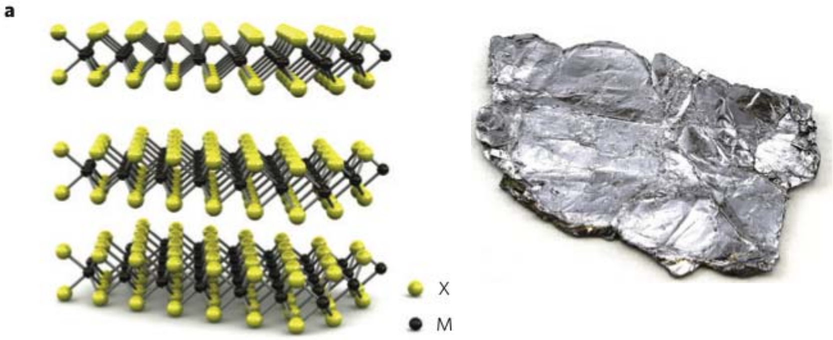

Wang et al. Nature Nanotech. 7 (2012) 699

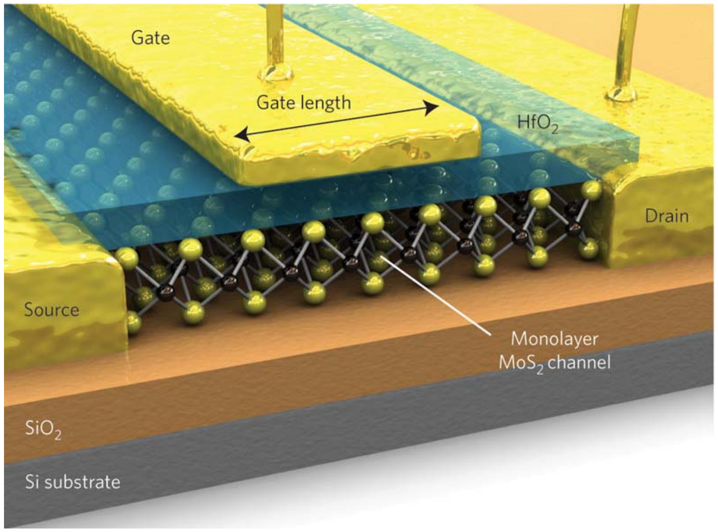

B. Radisavljevic et al. Nature Nanotech. **6** (2011)

TMD Potential Attributes for “Beyond CMOS”

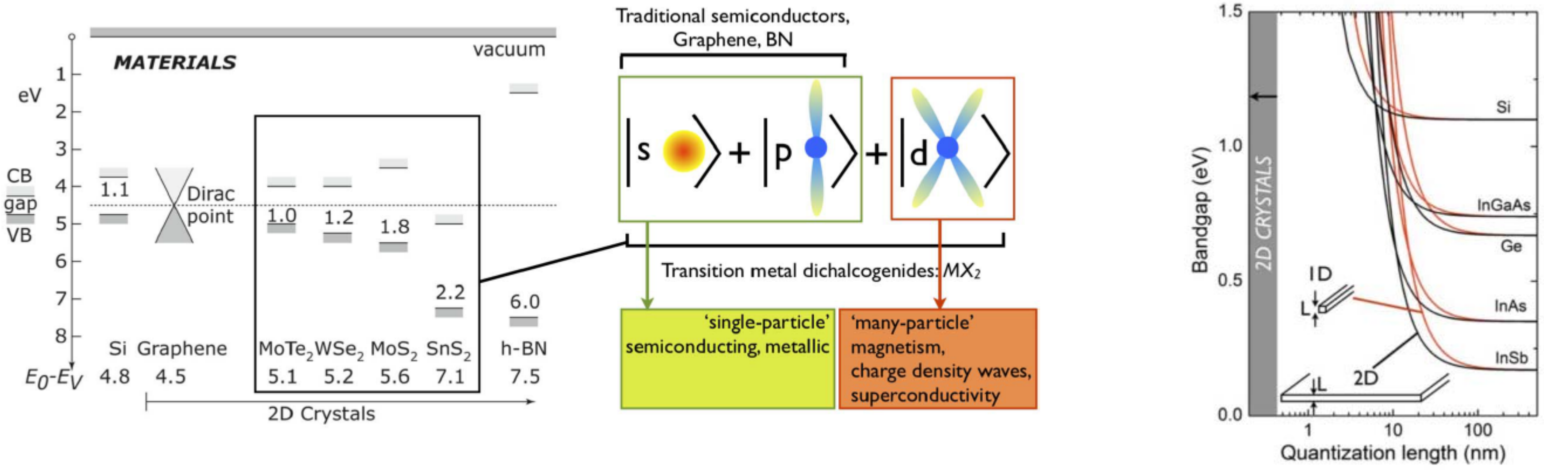

- Limited quantization effects for single layer channels
- Useful effective masses, bandgaps, and band offsets for transistors
- Full penetration of electric field through layer
- Anticipated dearth of defects like dangling bonds anticipated
- TMD Combinations + *d* orbitals anticipated to enable new functionalities

D. Jena, *Proc. IEEE* 101 (2013) 1585

A long history on TMD research…

Table 1
Layered materials conference series titles with book chapters covering layered materials research from 1976–2000.

Physics and chemistry of materials with low-dimension structures
(Previously published under the series title: physics and chemistry of materials with layered structures)

1. R.M.A. Lieth (Ed.): *Preparation and Crystal Growth of Materials with Layered Structures*. 1977
ISBN 90-277-0638-7
2. F. Levy (Ed.): *Crystallography and Crystal Chemistry of Materials with Layered Structures* 1976
ISBN 90-277-0586-0
3. T.J. Wieting and M. Schluter (eds.): *Electrons and Phonons in Layered Crystal Structures*.1979
ISBN 90-277-0897-5
4. P.A. Lee (Ed.): *Optical and Electrical Properties*. 1976
ISBN 90-277-0676-X
5. F. Hulliger: *Structural Chemistry of Layer-Type Phases*. Ed. by F. Levy. 1976
ISBN 90-277-0714-6
6. F. Levy (Ed.): *Intercalated Layered Materials*. 1979
ISBN 90-277-0967-X

Physics and chemistry of materials with low-dimensional structures series a: layered structures
7. V. Grasso (Ed.): *Electronic Structure and Electronic Transitions in Layered Materials*. 1986
ISBN 90-277-2102-5
8. K. Motizuki (ed.): *Structural Phase Transitions in Layered Transition Metal Compounds*. 1986
ISBN 90-277-2171-8
9. L.J. de Jongh (ed.): *Magnetic Properties of Layered Transition Metal Compounds*. 1990
ISBN 0-7923-0238-9
10. E. Doni, R. Girlanda, G. Pastori Parravicini and A. Quattropani (eds.): *Progress in Electron Properties of Solids*. Festschrift in Honour of Franco Bassani. 1989
ISBN 0-7923-0337-7
11. C. Schlenker (Ed.): *Low-Dimensional Electronic Properties of Molybdenum Bronzes and Oxides*. 1989 ISBN 0-7923-0085-8
12. Not published.
13. H. Aoki, M. Tsukada, M. Schluter and F. Levy (eds.): *New Horizons in Low-Dimensional Electron Systems*. A Festschrift in Honour of Professor H. Kamimura. 1992
ISBN 0-7923-1302-X
14. A. Aruchamy (Ed.): *Photoelectrochemistry and Photovoltaics of Layered Semiconductors*. 1992 ISBN 0-7923-1556-1
15. T. Butz (Ed.): *Nuclear Spectroscopy on Charge Density Wave Systems*. 1992
ISBN 0-7923-1779-3
16. G. Benedek (Ed.): *Surface Properties of Layered Structures*. 1992
ISBN 0-7923-1961-3
17. W. Muller-Warmuth and R. Schollhom (eds.): *Progress in Intercalation Research*. 1994
ISBN 0-7923-2357-2
18. L.J. de Jongh (Ed.): *Physics and Chemistry of Metal Cluster Compounds. Model Systems for Small Metal Particles*. 1994
ISBN 0-7923-2715-2
19. E.Y. Andrei (Ed.): *Two-Dimensional Electron Systems. On Helium and other Cryogenic Substrates*. 1997 ISBN 0-7923-4738-2
20. A. Furrer: *Neutron Scattering in Layered Copper-Oxide Superconductors*. 1998
ISBN 0-7923-5226-2
21. R.B. Heimann, S.E. Evsyukov and L. Kavan (eds.): *Carbyne and Carbynoid Structures*. 1999
ISBN 0-7923-5323-4
22. F.W. Boswell and J.C. Bennett (eds.): *Advances in the Crystallographic and Microstructural Analysis of Charge Density Wave Modulated Crystals*. 1999
ISBN 0-7923-5604-7
23. W. Andreoni (Ed.): *The Physics of Fullerene-Based and Fullerene-Related Materials*. 2000
ISBN 0-7923-6234-9
24. H.P. Hughes and H.I. Stamberg (eds.): *Electron Spectroscopies Applied to Low-Dimensional Structures*. 2000
ISBN 0-7923-6526-7

J. Appl. Physics 37 (1966) 1928

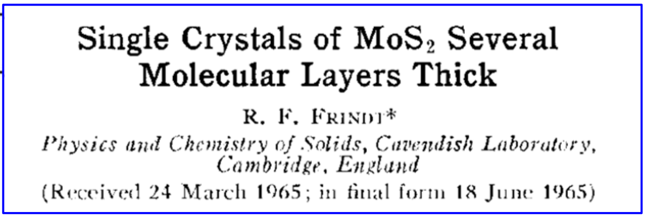

Single Crystals of MoS_2 Several Molecular Layers Thick

R. F. Frindt*
Physics and Chemistry of Solids, Cavendish Laboratory, Cambridge, England
(Received 24 March 1965; in final form 18 June 1965)

Adv. Physics 18 (1969) 193-335

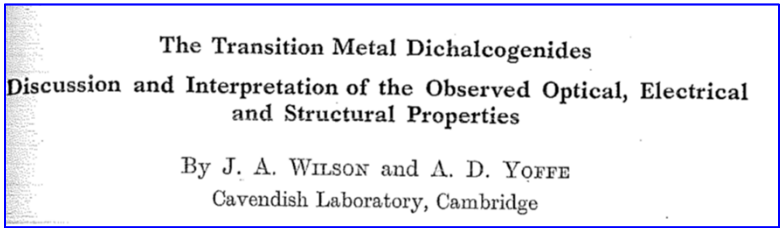

The Transition Metal Dichalcogenides
Discussion and Interpretation of the Observed Optical, Electrical and Structural Properties

By J. A. Wilson and A. D. Yoffe
Cavendish Laboratory, Cambridge

Prog. Surf. Sci. 29 (1988) 1-167

INTERFACIAL PROPERTIES OF SEMICONDUCTING TRANSITION METAL CHALCOGENIDES

W. JAEGERMANN and H. TRIBUTSCH

Hahn-Meitner-Institut, Bereich S
Glienicker Str. 100, D-1000 Berlin 39, Germany

Thin Solid Films **616**, 482 (2016)

TMD Potential Attributes for “Beyond CMOS”

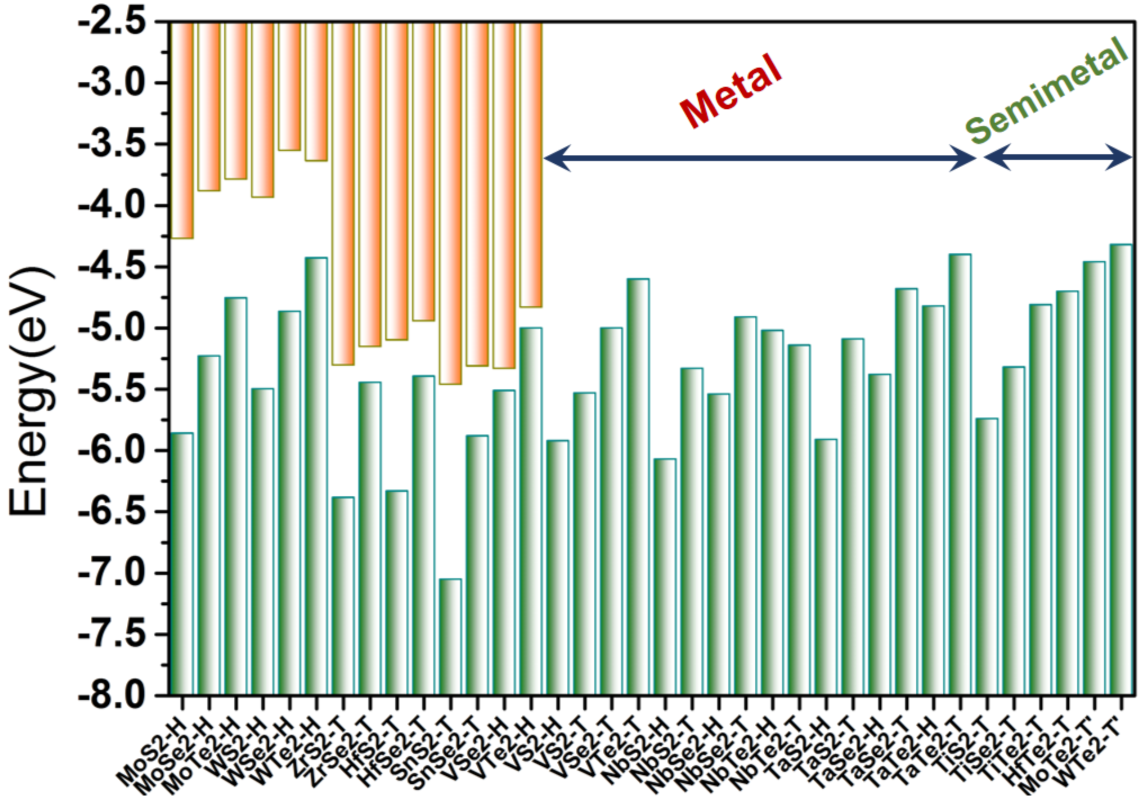

- Useful band structure for TFET heterostructure transistors
- Metal and semi-metal properties
- Applications in Nanoelectronics, Optoelectronics, Photovoltaics, and Photocatalysis

See also: C. Gong *et al*. APL 103 (5), 053513 (2013); APL 107 (2015) 139904

C. Zhang, et al., *2D Materials*, 4, 015026 (2017)

Interfaces and defects

Steep slope switching: The Effect of Interface Traps

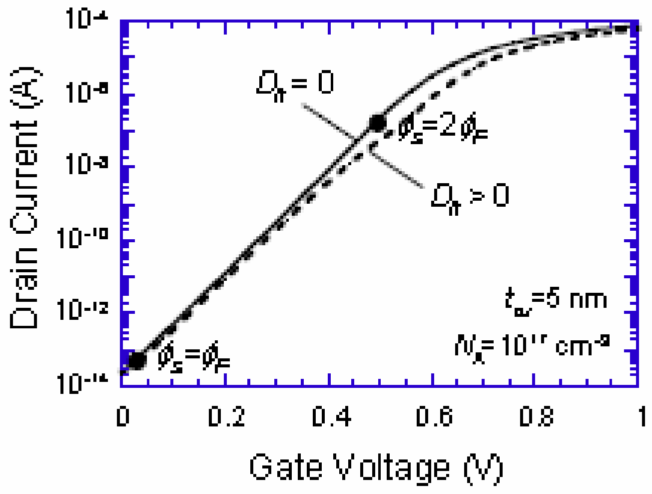

Fig. 26 Theoretical I_D-V_G curves for D_{it}=0 and $D_{it,min}$=2.7x10^{10} cm^{-2}eV^{-1}.

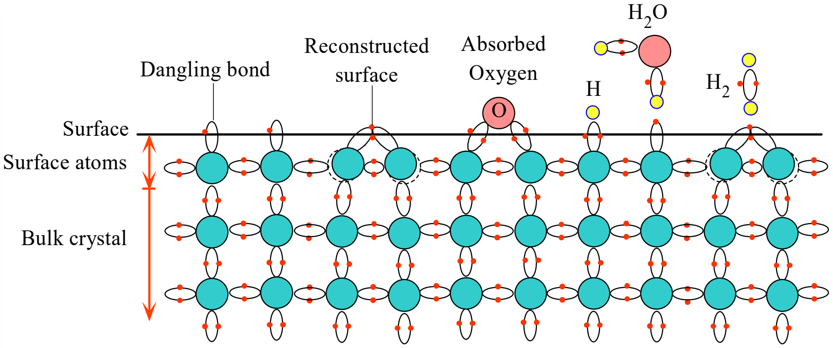

At the surface of a hypothetical two dimensional crystal, the atoms cannot fulfill their bonding requirements and therefore have broken, or dangling, bonds. Some of the surface atoms bond with each other; the surface becomes reconstructed. The surface can have physisorbed and chemisorbed atoms.

From *Principles of Electronic Materials and Devices, Third Edition*, S.O. Kasap (© McGraw-Hill, 2005)

Subthreshold swing “SS”: gate voltage required to change the I_D by one decade

$$SS = \frac{\partial V_g}{\partial(\log I_d)} = \underbrace{\frac{\partial V_g}{\partial \psi_s}}_{\text{Body factor}} \underbrace{\frac{\partial \psi_s}{\partial(\log I_d)}}_{\text{Carrier injection mechanism}} = \frac{\ln(10)kT}{q}\left[1+\frac{C_{bulk}+C_{it}}{C_{ox}}\right] \approx \frac{60T(K)}{300}\left[1+\frac{C_{bulk}+C_{it}}{C_{ox}}\right]$$

See e.g. Schroder (2009); Ionescu, et al. Nature 479 (2011) 329-337

Interfaces and defects

Steep slope switching: The Effect of Interface Traps

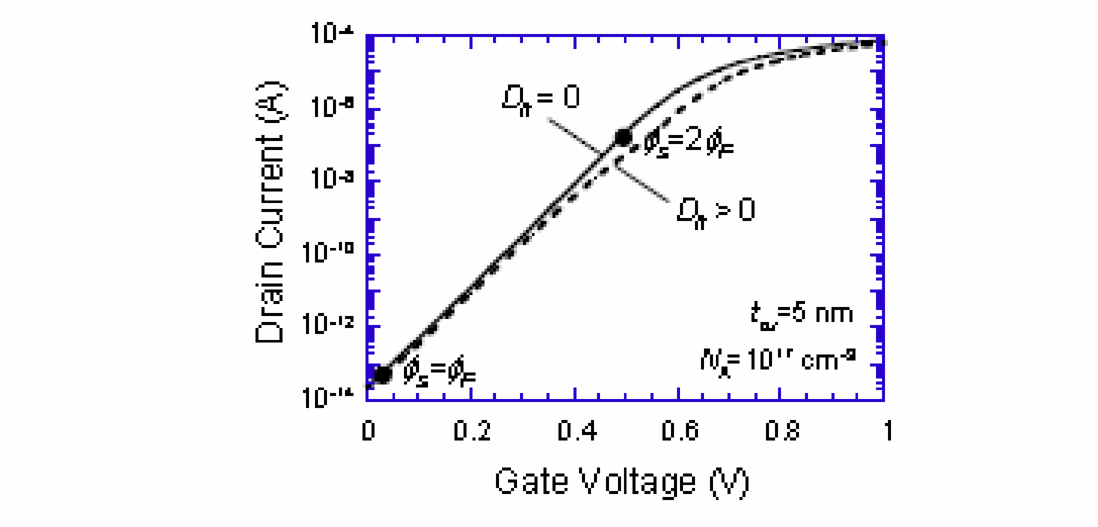

Fig. 26 Theoretical I_D-V_G curves for D_{it}=0 and $D_{it,min}$=2.7x10^{10} cm^{-2}eV^{-1}.

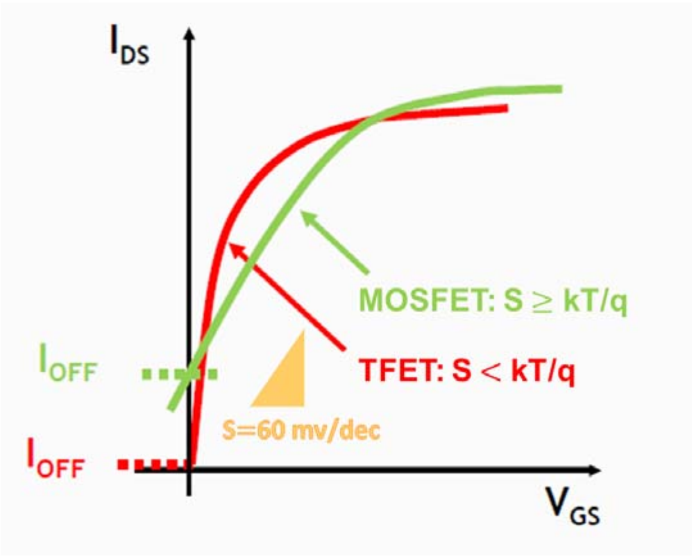

Subthreshold swing "SS": gate voltage required to change the I_D by one decade

$$SS = \frac{\partial V_g}{\partial(\log I_d)} = \underbrace{\frac{\partial V_g}{\partial \psi_s}}_{\text{Body factor}} \underbrace{\frac{\partial \psi_s}{\partial(\log I_d)}}_{\text{Carrier injection mechanism}} = \frac{\ln(10)kT}{q}\left[1 + \frac{C_{bulk} + C_{it}}{C_{ox}}\right] \approx \frac{60T(K)}{300}\left[1 + \frac{C_{bulk} + C_{it}}{C_{ox}}\right]$$

See e.g. Schroder (2009); Ionescu, et al. Nature 479 (2011) 329-337

UT DALLAS

Recall the Si/SiO_2 interface…

Orientation and (Intrinsic) Interface State Density

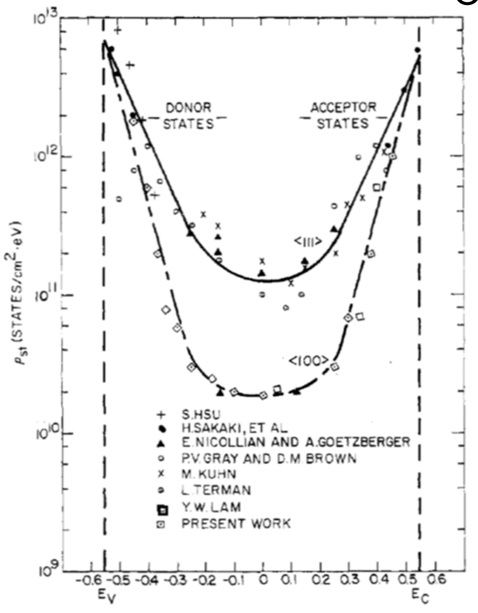

Fig. 3. Interface state density in the Si–SiO_2 system.

White and Cricchi, IEEE TED 19(12), 1280 (1972)

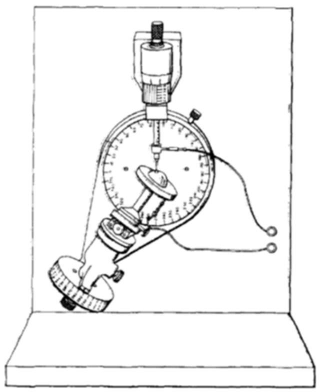

Fig. 1. Goniometer used for measuring the MOS capacitance and ac conductance on the surface of the oxidized silicon hemisphere. The hemisphere can be rotated to place any desired surface orientation under the stationary mercury-drop field electrode.

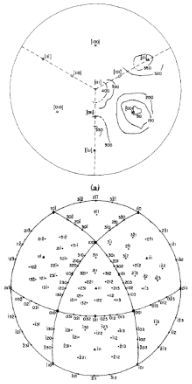

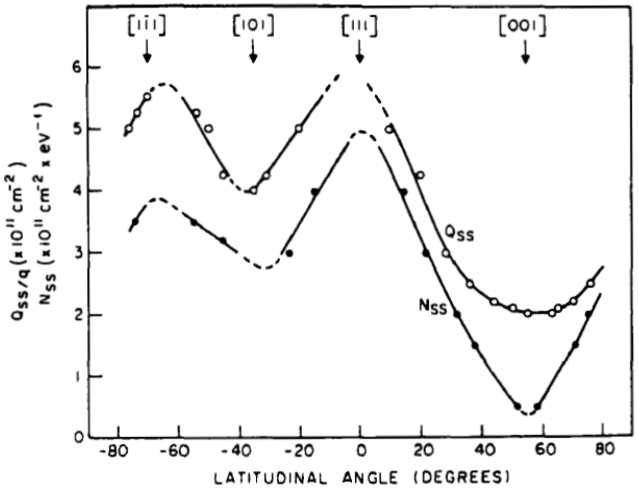

Arnold, *et al.*, APL 13(12) 413(1968)
Abowitz, *et al.*, PRL 18, 543 (1967)

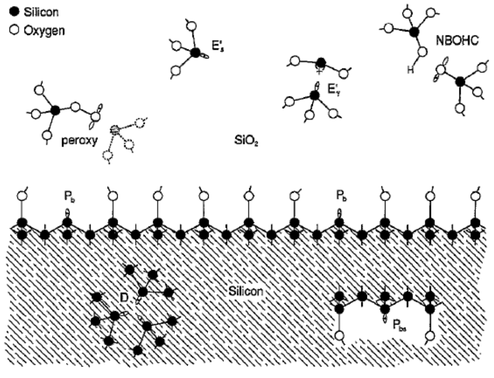

Figure 11. Paramagnetic point defects observed in Si–SiO_2 structures by electron spin resonance.

Helms and Poindexter, Rep.Prog.Phys. 57, 791 (1994)

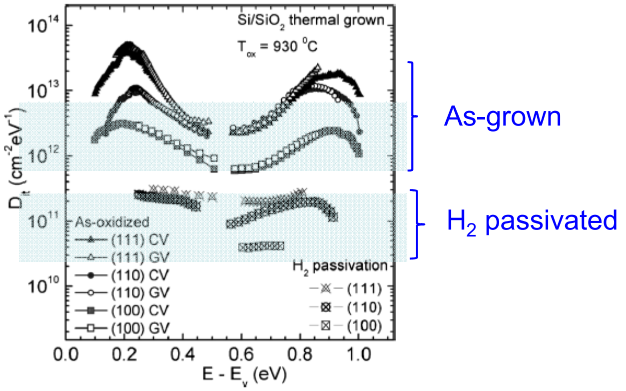

FIG. 3. $D_{it}(E)$ profiles of Si/SiO_2 interfaces derived from the CV (solid symbols) and GV (open symbols) methods in Si/SiO_2 samples fabricated on (100), (110), and (111) faces of Si. Results are shown for both the as-oxidized samples (no H-passivation) and those subjected to H_2 passivation (30 min anneal in 1.1 atm H_2 at 400 °C).

Thoan, *et al.*, J. Appl. Phys. 109, 013710 (2011)

Recall the Si/SiO_2 interface…

Intrinsic Interface Defects

- Si(100) surface orientation provides the lowest theoretical dangling bond density (reactivity)
  - Density Si(100) = 6.8×10^{14} /cm^2
  - Density Si(111) = 11.8×10^{14} /cm^2
  - Density Si(110) = 9.6×10^{14} /cm^2
- Dangling bonds (“P_b”) provide a dominant defect population
  - As-grown interfaces can have densities $\geq10^{12}$/cm^2
- Passivation of dangling bonds by hydrogen is effective
  - Density can be reduced to ~5×10^{10}/cm^2
- Detection by sensitive characterization techniques
  - Surfaces: Thermal Desorption, FTIR, LEED, STS, PES, etc.
  - Devices: Spin Resonance, Capacitance-Voltage, Transistors, etc.
- Detection of defects in SiO_2 bonding as well
  - Strained bonds, dangling bonds (E’), peroxy bonding, hydroxyls, etc.
  - Depends on growth T, stoichiometry, charge injection, radiation, etc.
  - Can be located near interfaces (channel or gate) or within bulk

2D Materials Challenges

- Large areas synthesis
  - As large as possible or perhaps selective growth and within CMOS thermal constraints
  - “Back End of Line” → $T_{max} = 500°C$
- High quality material
  - Uniform, continuous/coalesced
  - Low defect density
  - Low impurity concentrations
  - High mobility
- Contacts
  - Doping control
  - Low contact resistance
- Etching
  - Atomic layer etching control

- Materials Challenges
- Tools and Methods
- TMDs
- Summary

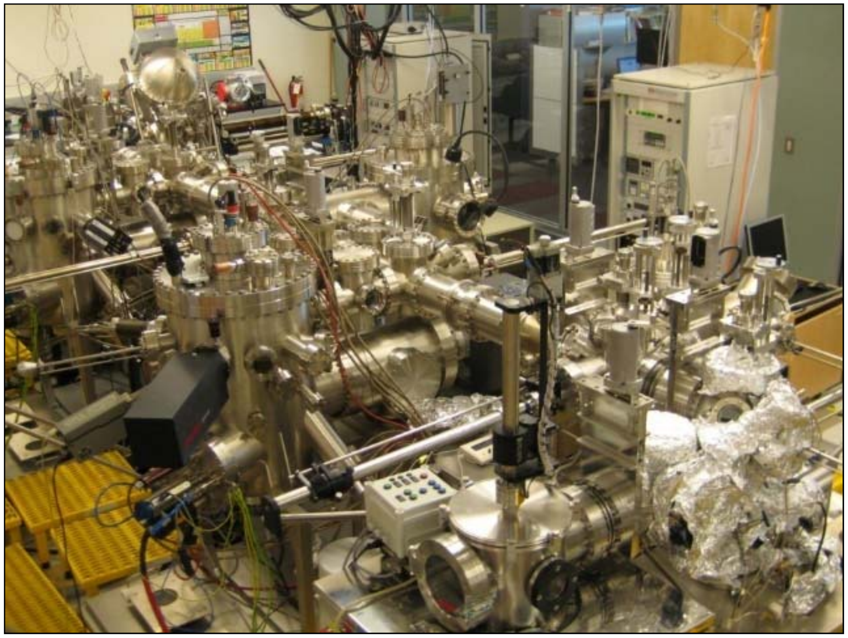

Tools for *in-situ* studies of interfaces…

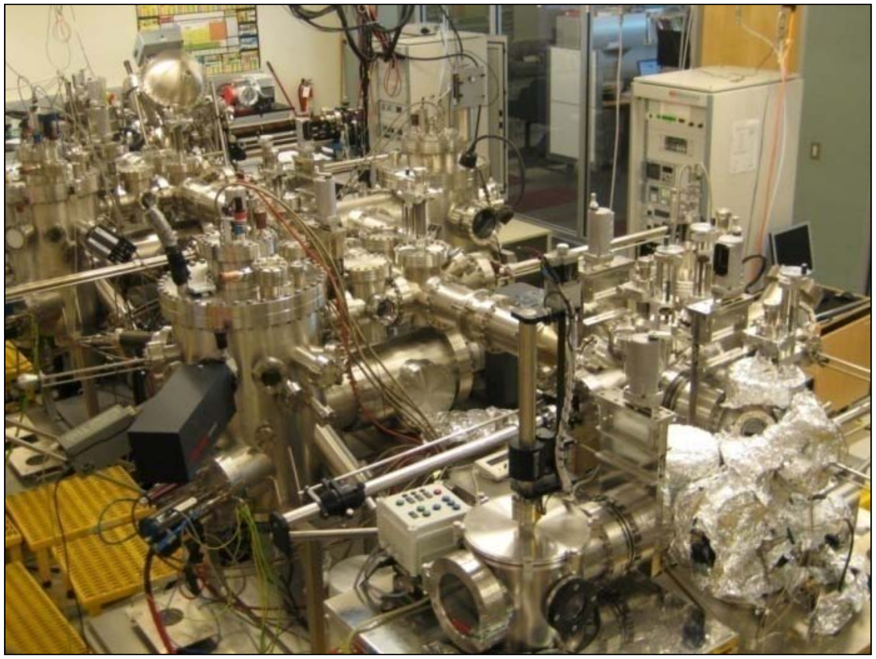

UHV Cluster System

UHV Surface Science System

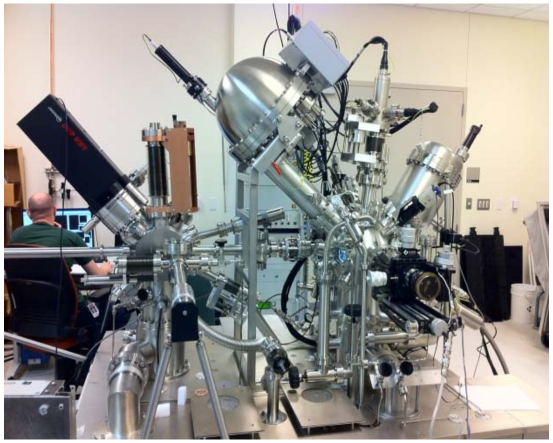

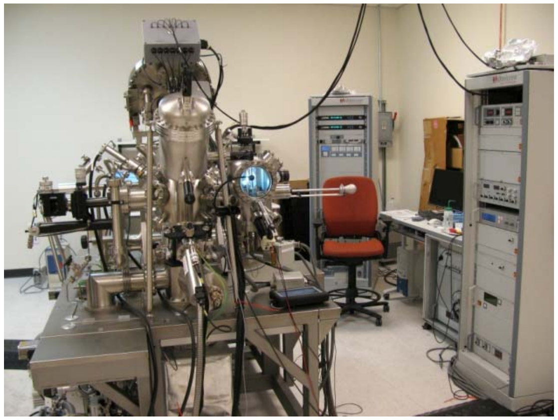

In-situ deposition and analysis system at UT-Dallas

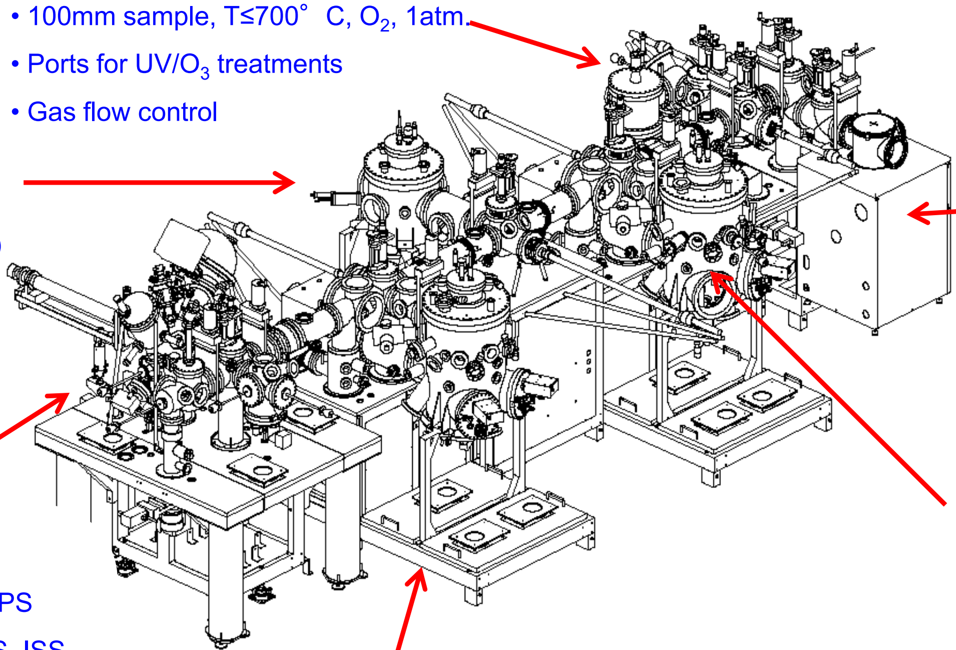

Sputter Module

- UHV capable
- 4 RF magnetrons
- Pressure/valve control
- Sample T≤1000° C (Pt)

Annealing Module

- Custom UHV furnace
- 100mm sample, T≤700° C, O_2, 1atm.
- Ports for UV/O_3 treatments
- Gas flow control

PEALD Module

- Hot wall reactor
- Custom UHV transfer system
- 100mm sample, T≤350° C
- Liquid, gas and solid sources
- Gas flow control

Analytical Module

- Monochromatic Al-Kα XPS
- High Intensity UPS, AES, ISS
- LEED
- Substrate size flexible
- 1000° C sample heater
- LN$_2$ sample cooling
- Sample rotation, ARXPS

MBE Module

- 2 e-gun hearths (Group IV – Si, Ge)
- P, As, Sb, B effusion cells
- 100mm wafer, T≤1200° C, shutter
- QMS (x-beam), quartz microbalance
- RHEED

Metal MBD Module

- 4 pocket e-gun hearth
- Sample heater (T≤1000° C)
- Effusion cells
- Atomic hydrogen source (H_2 cracker)
- RHEED

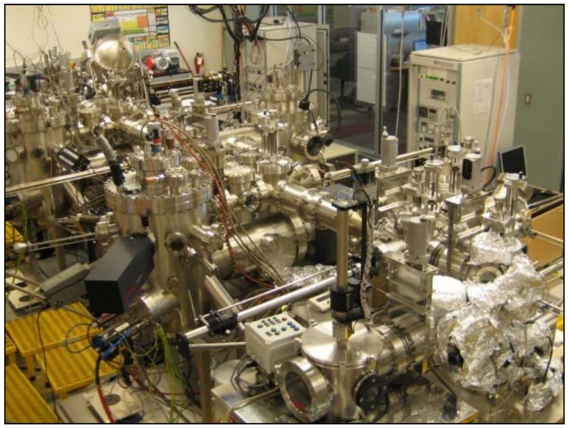

Example: ALD Tool Integration

Remote Plasma-Enhanced R200 ALD Reactor at UT-Dallas

Picosun
The ALD Powerhouse

UT DALLAS

In-situ half cycle ALD reactions study by XPS

High Resolution Monochromatic XPS

Picosun PEALD
Hot wall and Shower head type

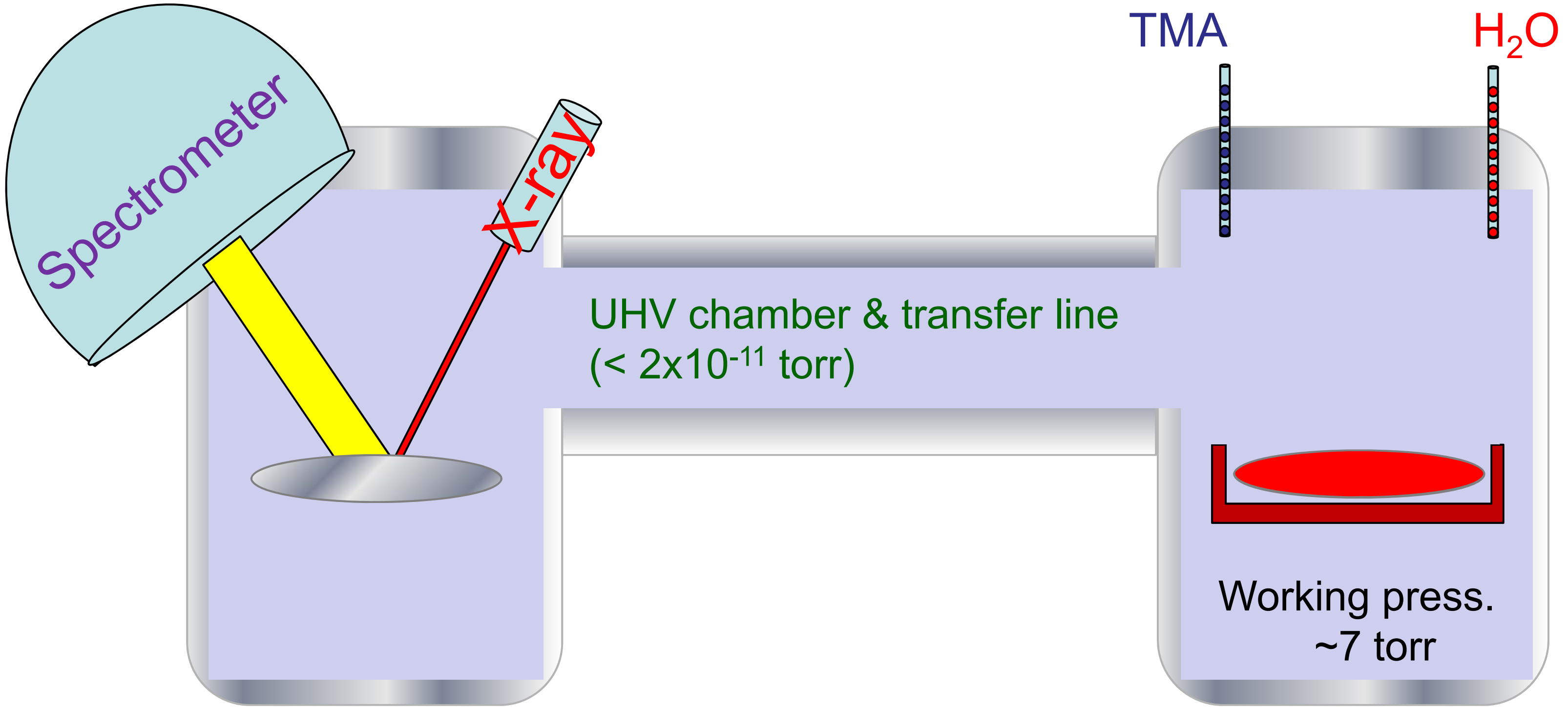

XPS Analysis

Pre-substrate Scan

Analysis after 1st Al pulse

Analysis after 1st H_2O pulse

ALD (Al & H_2O)

Al pulse

H_2O pulse

UHV Surface Science System

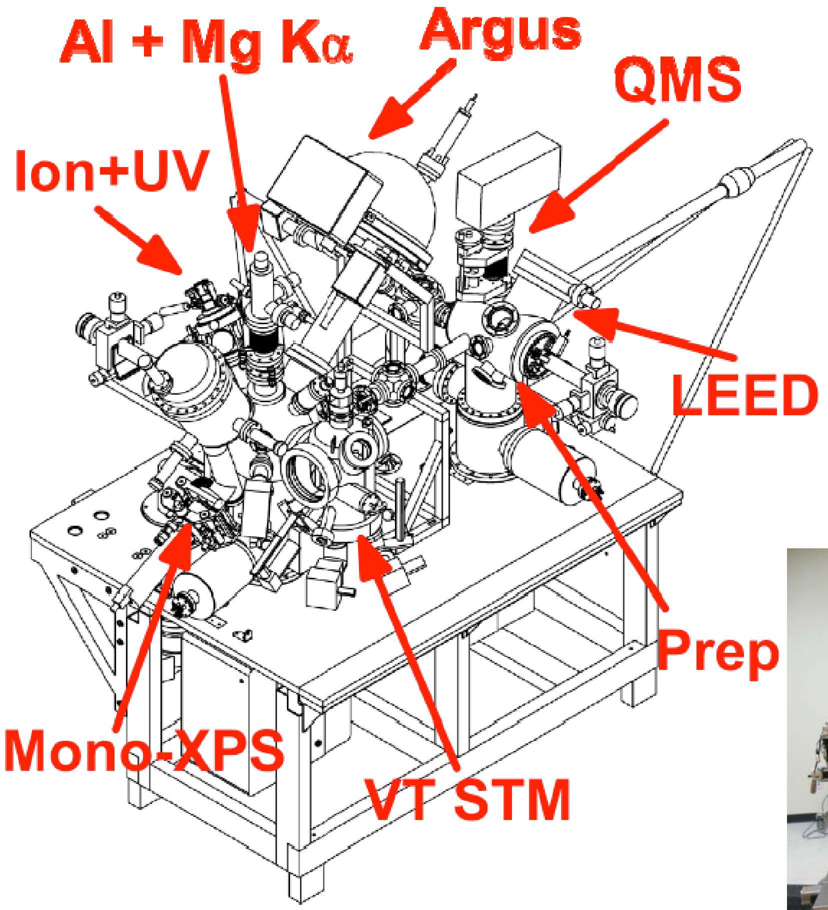

- Variable Temperature STM/AFM
- Monochromatic XPS with Argus 128 channel detection
- Twin Anode X-ray Source
- UPS – valence band studies
- Thermal Desorption Spectroscopy
- Low Energy Electron Diffraction
- Effusion/e-beam deposition

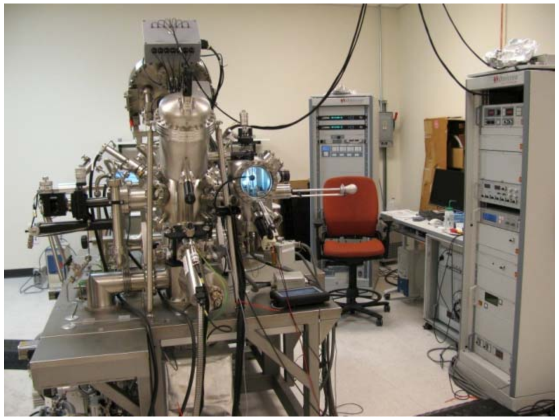

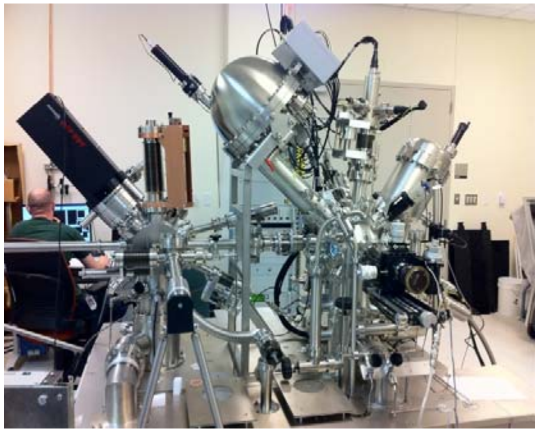

ECS Transactions, **64** (9) 109-116 (2014)

Sensitivity of Characterization Methods

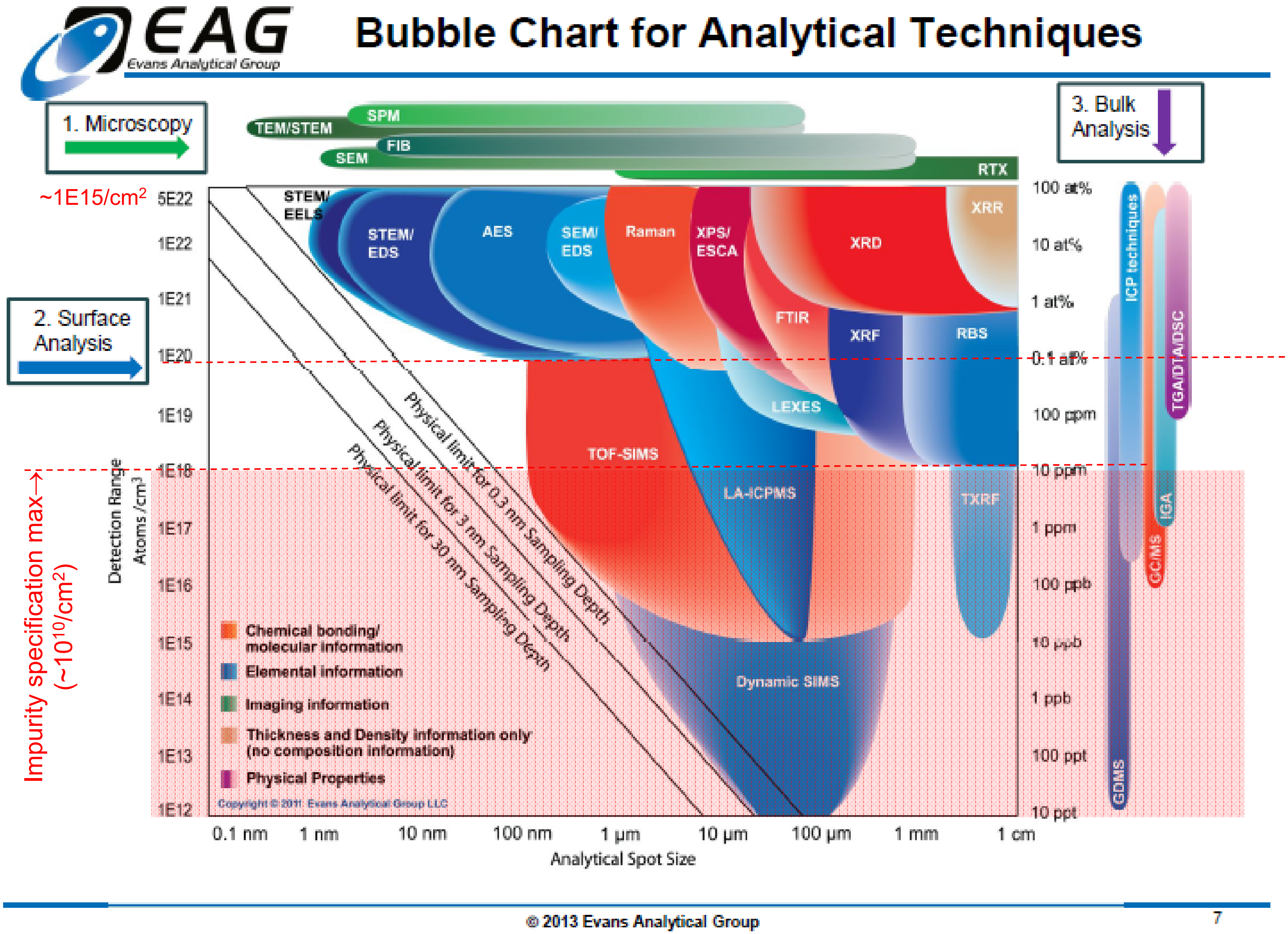

See: http://www.eag.com/mc/analytical-techniques.html

- Materials Challenges
- Methods
- TMDs
    - Impurities
- Summary

ICPMS of Extrinsic Impurities on MoS$_2$

MoS$_2$ from Australian source ‘**a-MoS$_2$**’

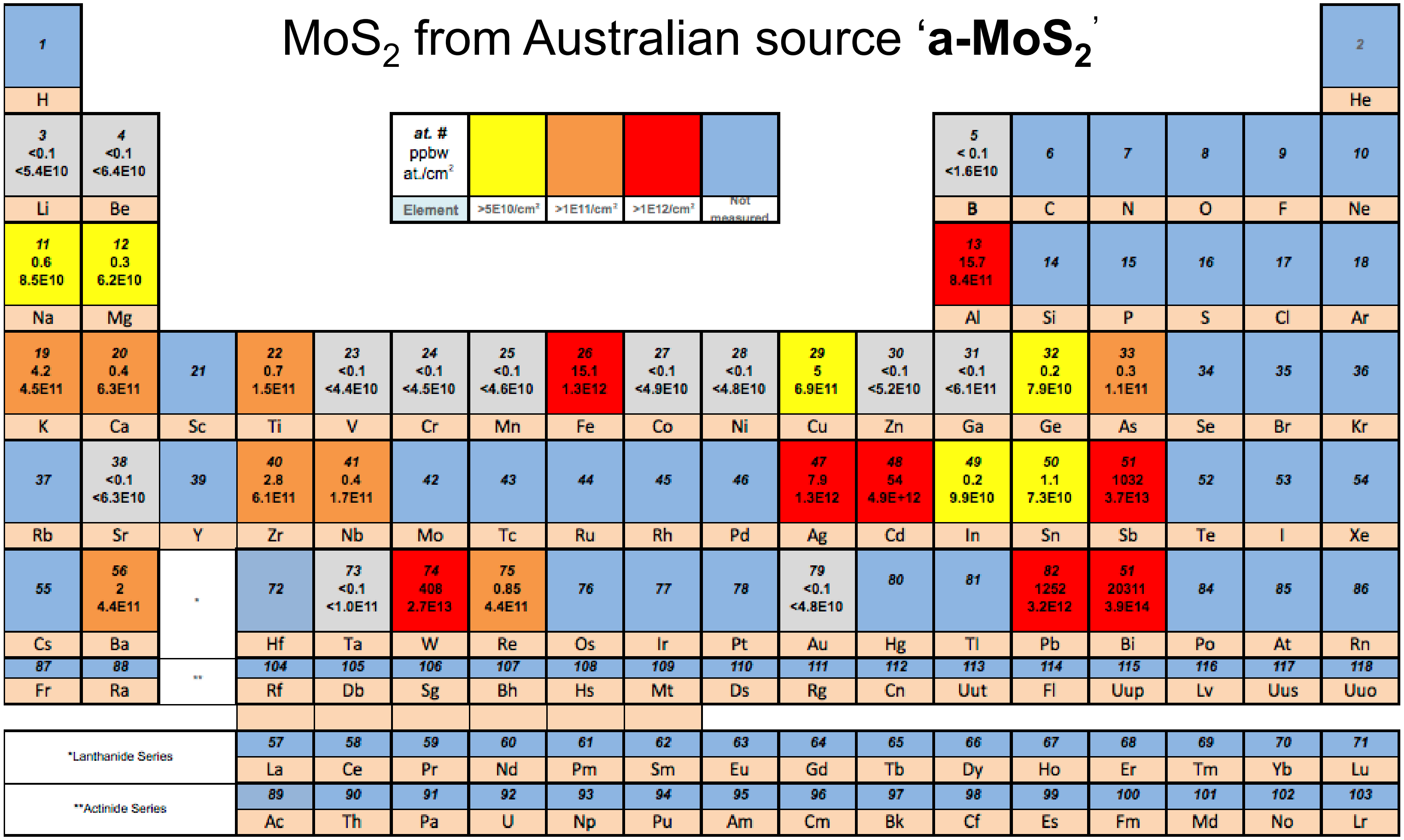

1 H																	2 He
3 <0.1 <5.4E10 Li	4 <0.1 <6.4E10 Be											5 < 0.1 <1.6E10 B	6 C	7 N	8 O	9 F	10 Ne
11 0.6 8.5E10 Na	12 0.3 6.2E10 Mg											13 15.7 8.4E11 Al	14 Si	15 P	16 S	17 Cl	18 Ar
19 4.2 4.5E11 K	20 0.4 6.3E11 Ca	21 Sc	22 0.7 1.5E11 Ti	23 <0.1 <4.4E10 V	24 <0.1 <4.5E10 Cr	25 <0.1 <4.6E10 Mn	26 15.1 1.3E12 Fe	27 <0.1 <4.9E10 Co	28 <0.1 <4.8E10 Ni	29 5 6.9E11 Cu	30 <0.1 <5.2E10 Zn	31 <0.1 <6.1E11 Ga	32 0.2 7.9E10 Ge	33 0.3 1.1E11 As	34 Se	35 Br	36 Kr
37 Rb	38 <0.1 <6.3E10 Sr	39 Y	40 2.8 6.1E11 Zr	41 0.4 1.7E11 Nb	42 Mo	43 Tc	44 Ru	45 Rh	46 Pd	47 7.9 1.3E12 Ag	48 54 4.9E+12 Cd	49 0.2 9.9E10 In	50 1.1 7.3E10 Sn	51 1032 3.7E13 Sb	52 Te	53 I	54 Xe
55 Cs	56 2 4.4E11 Ba	*	72 Hf	73 <0.1 <1.0E11 Ta	74 408 2.7E13 W	75 0.85 4.4E11 Re	76 Os	77 Ir	78 Pt	79 <0.1 <4.8E10 Au	80 Hg	81 Tl	82 1252 3.2E12 Pb	51 20311 3.9E14 Bi	84 Po	85 At	86 Rn
87 Fr	88 Ra	**	104 Rf	105 Db	106 Sg	107 Bh	108 Hs	109 Mt	110 Ds	111 Rg	112 Cn	113 Uut	114 Fl	115 Uup	116 Lv	117 Uus	118 Uuo

*Lanthanide Series	57 La	58 Ce	59 Pr	60 Nd	61 Pm	62 Sm	63 Eu	64 Gd	65 Tb	66 Dy	67 Ho	68 Er	69 Tm	70 Yb	71 Lu
**Actinide Series	89 Ac	90 Th	91 Pa	92 U	93 Np	94 Pu	95 Am	96 Cm	97 Bk	98 Cf	99 Es	100 Fm	101 Md	102 No	103 Lr

at. # ppbw at./cm^2	🟨	🟧	🟥	🟦
Element	>5E10/cm^2	>1E11/cm^2	>1E12/cm^2	Not measured

- Vapor ICPMS utilized by commercial laboratory
- “Digestion” here entails only surface region impurities
- Element list mainly based on Si-industry relevant impurity species – i.e. impurities that induce levels in the band gap

R. Addou *et al.* ACS Nano, 9, 9124 (2015)

UT DALLAS

ICPMS of Extrinsic Impurities on MoS_2

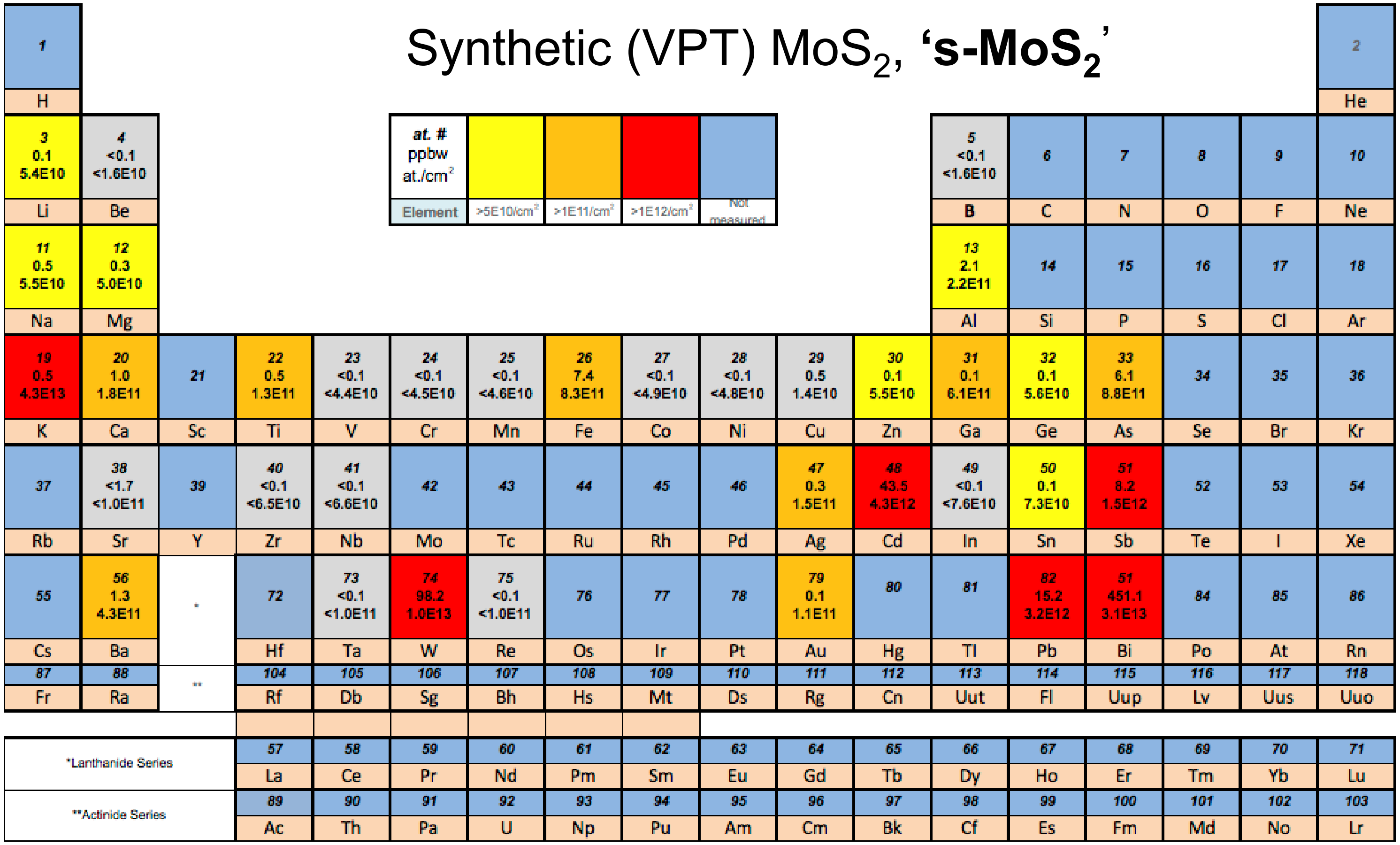

Synthetic (VPT) MoS_2, **'s-MoS_2'**

at. # ppbw at./cm^2	🟨	🟧	🟥	🟦
Element	>5E10/cm^2	>1E11/cm^2	>1E12/cm^2	Not measured

1 H																	2 He
3 0.1 5.4E10 Li	4 <0.1 <1.6E10 Be											5 <0.1 <1.6E10 B	6 C	7 N	8 O	9 F	10 Ne
11 0.5 5.5E10 Na	12 0.3 5.0E10 Mg											13 2.1 2.2E11 Al	14 Si	15 P	16 S	17 Cl	18 Ar
19 0.5 4.3E13 K	20 1.0 1.8E11 Ca	21 Sc	22 0.5 1.3E11 Ti	23 <0.1 <4.4E10 V	24 <0.1 <4.5E10 Cr	25 <0.1 <4.6E10 Mn	26 7.4 8.3E11 Fe	27 <0.1 <4.9E10 Co	28 <0.1 <4.8E10 Ni	29 0.5 1.4E10 Cu	30 0.1 5.5E10 Zn	31 0.1 6.1E11 Ga	32 0.1 5.6E10 Ge	33 6.1 8.8E11 As	34 Se	35 Br	36 Kr
37 Rb	38 <1.7 <1.0E11 Sr	39 Y	40 <0.1 <6.5E10 Zr	41 <0.1 <6.6E10 Nb	42 Mo	43 Tc	44 Ru	45 Rh	46 Pd	47 0.3 1.5E11 Ag	48 43.5 4.3E12 Cd	49 <0.1 <7.6E10 In	50 0.1 7.3E10 Sn	51 8.2 1.5E12 Sb	52 Te	53 I	54 Xe
55 Cs	56 1.3 4.3E11 Ba	*	72 Hf	73 <0.1 <1.0E11 Ta	74 98.2 1.0E13 W	75 <0.1 <1.0E11 Re	76 Os	77 Ir	78 Pt	79 0.1 1.1E11 Au	80 Hg	81 Tl	82 15.2 3.2E12 Pb	51 451.1 3.1E13 Bi	84 Po	85 At	86 Rn
87 Fr	88 Ra	**	104 Rf	105 Db	106 Sg	107 Bh	108 Hs	109 Mt	110 Ds	111 Rg	112 Cn	113 Uut	114 Fl	115 Uup	116 Lv	117 Uus	118 Uuo

*Lanthanide Series	57 La	58 Ce	59 Pr	60 Nd	61 Pm	62 Sm	63 Eu	64 Gd	65 Tb	66 Dy	67 Ho	68 Er	69 Tm	70 Yb	71 Lu
**Actinide Series	89 Ac	90 Th	91 Pa	92 U	93 Np	94 Pu	95 Am	96 Cm	97 Bk	98 Cf	99 Es	100 Fm	101 Md	102 No	103 Lr

- Impurity concentration easily exceed $5\times10^{10}/cm^2$.
- Many impurities have energy levels within the bandgap of silicon.
- Presence of ionized impurities is expected to have a high impact in carrier transport measurements

R. Addou *et al.* ACS Nano, 9, 9124 (2015)

XPS of Extrinsic Impurities on MoS_2

As expected, many below the limit of detection!

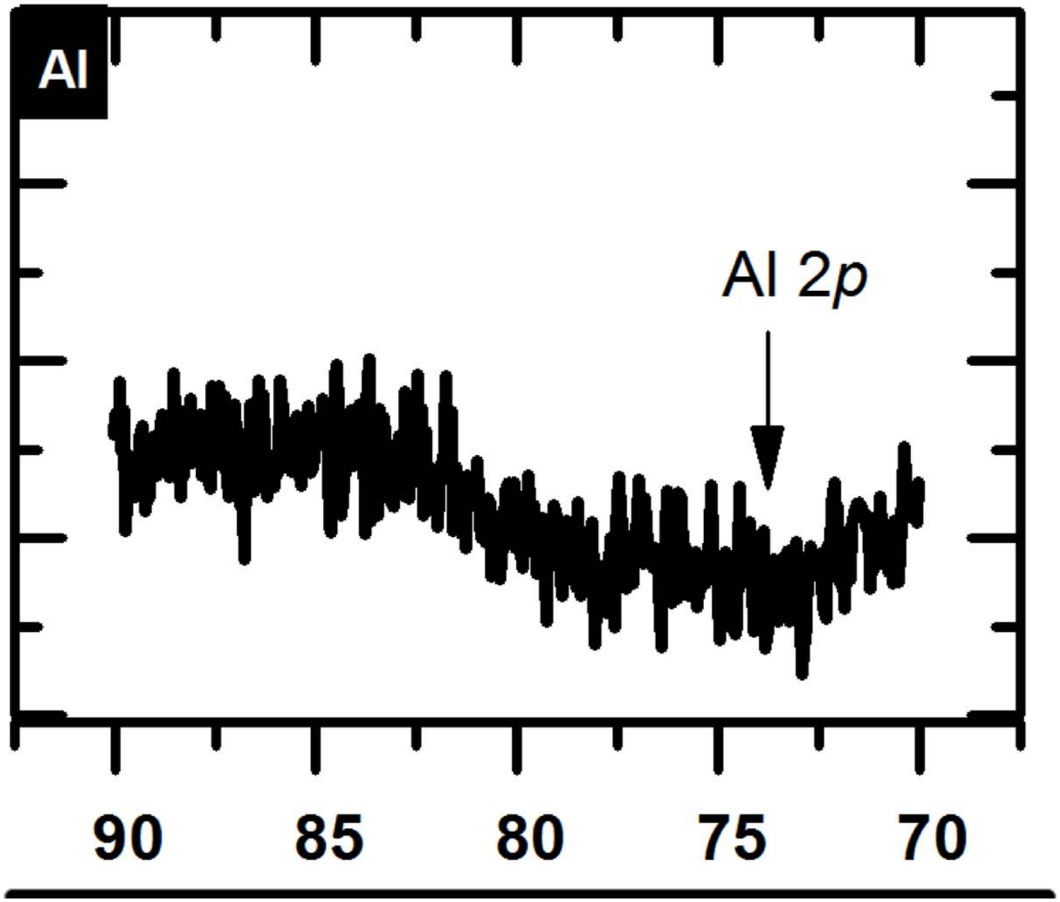

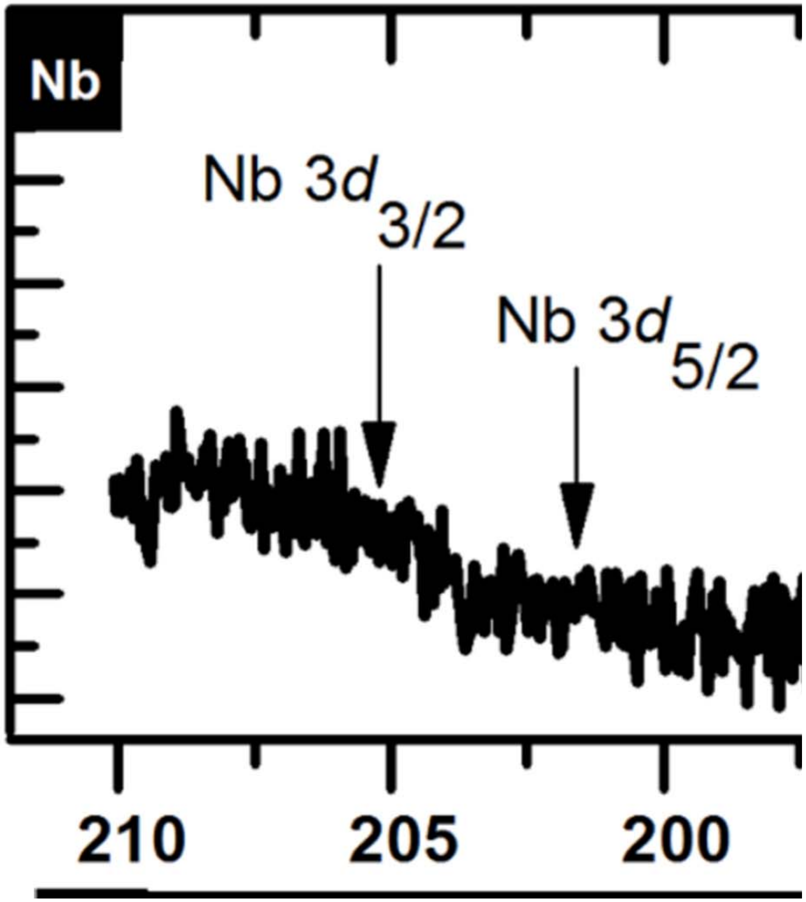

- Impurity concentration easily exceed $5\times10^{10}/cm^2$.
- Sensitivity of the characterization method is essential
- Incorrect to state “No Impurities”…

R. Addou *et al.* ACS Nano, 9, 9124 (2015)

MoS_2: Impurity Effect Estimate

- Theory →Impurities must be kept well below $10^{12}/cm^2$

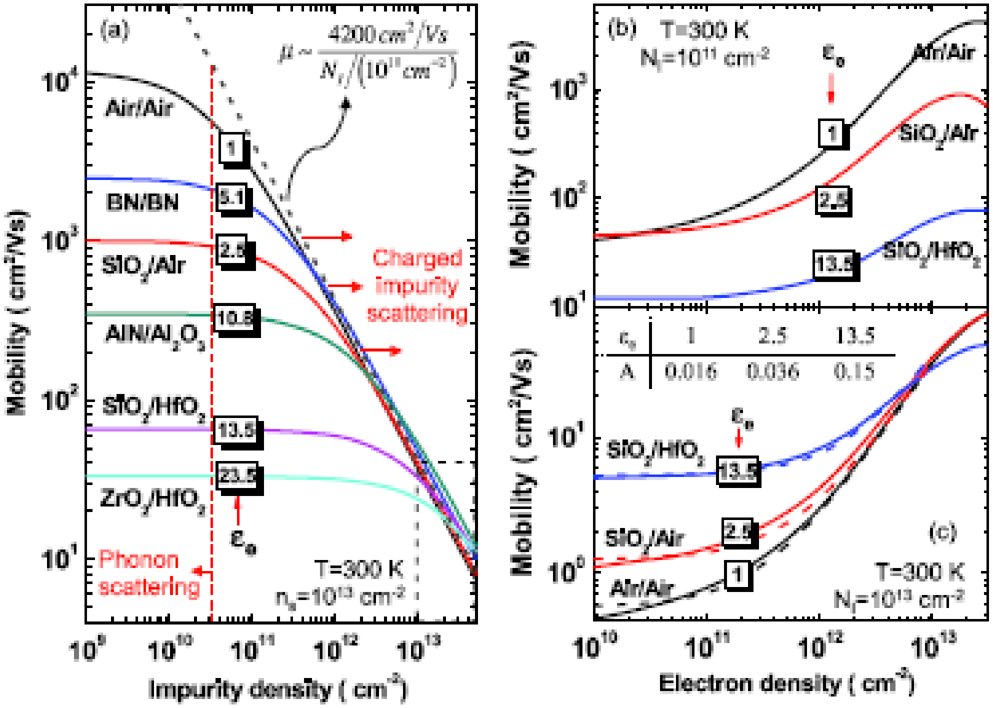

FIG. 7. The room-temperature net electron mobilities in SL MoS_2, considering all kinds of scattering mechanisms as a function of (a) N_I with fixed n_s at 10^{13} cm^{-2}; (b) and (c) n_s with N_I fixing at 10^{11} and 10^{13} cm^{-2}, respectively. The numbers on the curves show the average dielectric constant of the surrounding dielectrics. Dashed lines show the fitted electron mobilities.

Ma and Jena, *Phys. Rev. X* 4 (2014) 011043

UT DALLAS

ICPMS Analysis of CVT WS_2

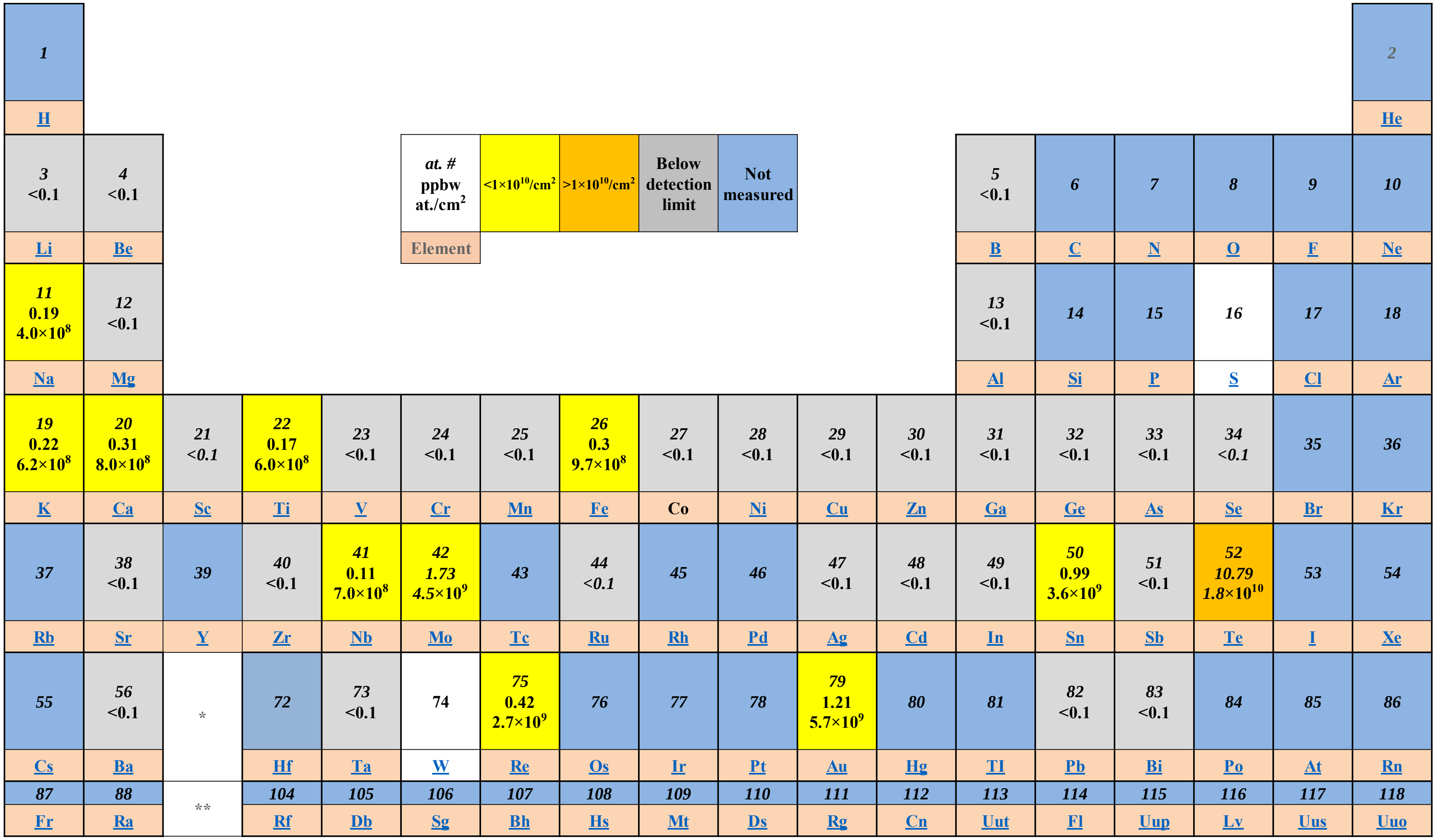

at. # ppbw at./cm^2 Element	<1×10^{10}/cm^2	>1×10^{10}/cm^2	Below detection limit	Not measured

1 H																	2 He
3 <0.1 Li	4 <0.1 Be											5 <0.1 B	6 C	7 N	8 O	9 F	10 Ne
11 0.19 4.0×10^{8} Na	12 <0.1 Mg											13 <0.1 Al	14 Si	15 P	16 S	17 Cl	18 Ar
19 0.22 6.2×10^{8} K	20 0.31 8.0×10^{8} Ca	21 <0.1 Sc	22 0.17 6.0×10^{8} Ti	23 <0.1 V	24 <0.1 Cr	25 <0.1 Mn	26 0.3 9.7×10^{8} Fe	27 <0.1 Co	28 <0.1 Ni	29 <0.1 Cu	30 <0.1 Zn	31 <0.1 Ga	32 <0.1 Ge	33 <0.1 As	34 <0.1 Se	35 Br	36 Kr
37 Rb	38 <0.1 Sr	39 Y	40 <0.1 Zr	41 0.11 7.0×10^{8} Nb	42 1.73 4.5×10^{9} Mo	43 Tc	44 <0.1 Ru	45 Rh	46 Pd	47 <0.1 Ag	48 <0.1 Cd	49 <0.1 In	50 0.99 3.6×10^{9} Sn	51 <0.1 Sb	52 10.79 1.8×10^{10} Te	53 I	54 Xe
55 Cs	56 <0.1 Ba	*	72 Hf	73 <0.1 Ta	74 W	75 0.42 2.7×10^{9} Re	76 Os	77 Ir	78 Pt	79 1.21 5.7×10^{9} Au	80 Hg	81 Tl	82 <0.1 Pb	83 <0.1 Bi	84 Po	85 At	86 Rn
87 Fr	88 Ra	**	104 Rf	105 Db	106 Sg	107 Bh	108 Hs	109 Mt	110 Ds	111 Rg	112 Cn	113 Uut	114 Fl	115 Uup	116 Lv	117 Uus	118 Uuo

- Impurity concentration kept below 5×10^{10}/cm^2.
- Better control of growth process and environment

Unpublished

ICPMS Analysis of CVT WSe_2

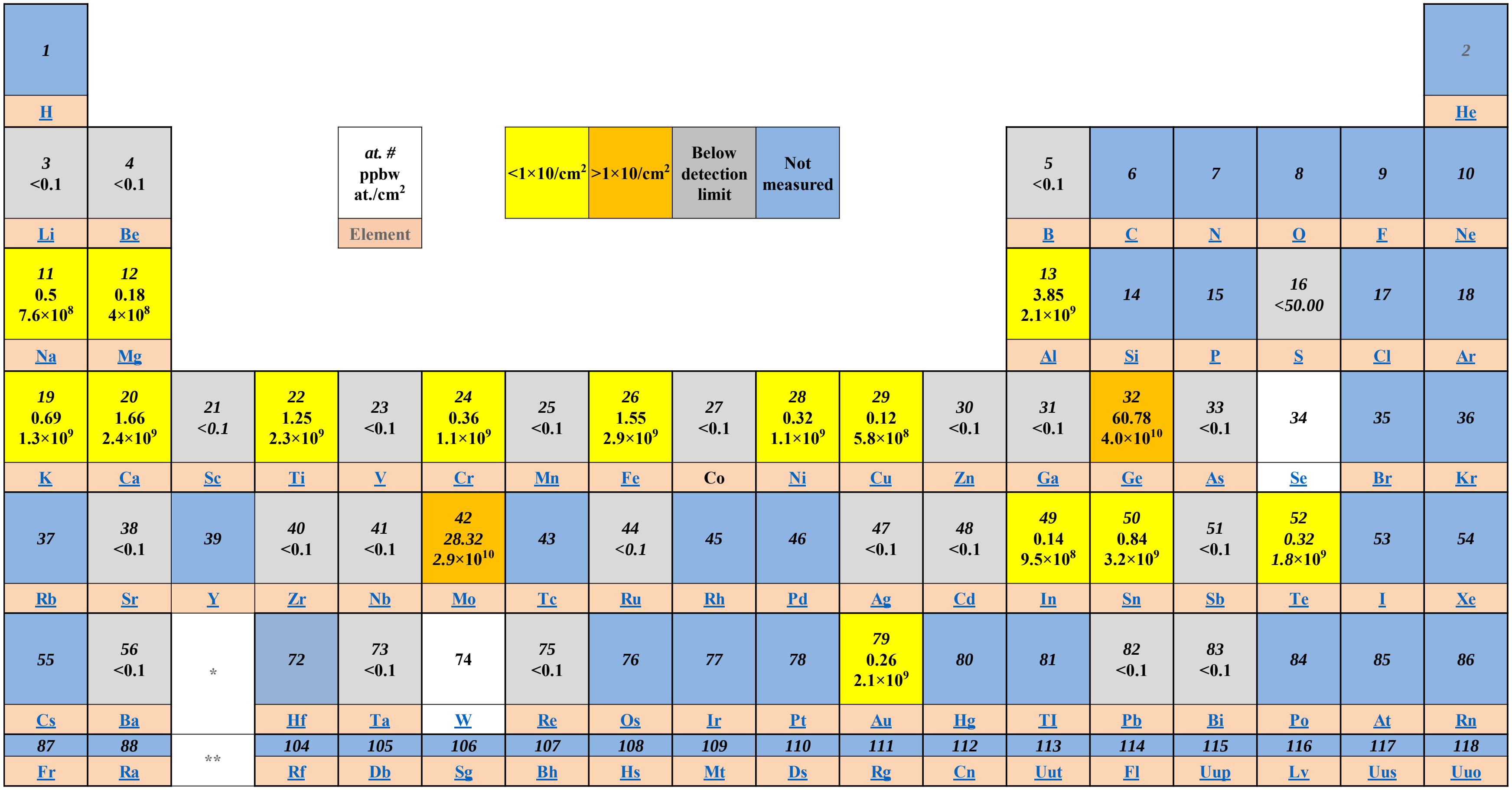

at. # ppbw at./cm^2 Element

$<1\times10/cm^2$	$>1\times10/cm^2$	Below detection limit	Not measured

1 H																	*2* He
3 <0.1 Li	*4* <0.1 Be											*5* <0.1 B	*6* C	*7* N	*8* O	*9* F	*10* Ne
11 0.5 7.6×10^{8} Na	*12* 0.18 4×10^{8} Mg											*13* 3.85 2.1×10^{9} Al	*14* Si	*15* P	*16* <50.00 S	*17* Cl	*18* Ar
19 0.69 1.3×10^{9} K	*20* 1.66 2.4×10^{9} Ca	*21* <0.1 Sc	*22* 1.25 2.3×10^{9} Ti	*23* <0.1 V	*24* 0.36 1.1×10^{9} Cr	*25* <0.1 Mn	*26* 1.55 2.9×10^{9} Fe	*27* <0.1 Co	*28* 0.32 1.1×10^{9} Ni	*29* 0.12 5.8×10^{8} Cu	*30* <0.1 Zn	*31* <0.1 Ga	*32* 60.78 4.0×10^{10} Ge	*33* <0.1 As	*34* Se	*35* Br	*36* Kr
37 Rb	*38* <0.1 Sr	*39* Y	*40* <0.1 Zr	*41* <0.1 Nb	*42* *28.32* 2.9×10^{10} Mo	*43* Tc	*44* *<0.1* Ru	*45* Rh	*46* Pd	*47* <0.1 Ag	*48* <0.1 Cd	*49* 0.14 9.5×10^{8} In	*50* 0.84 3.2×10^{9} Sn	*51* <0.1 Sb	*52* *0.32* 1.8×10^{9} Te	*53* I	*54* Xe
55 Cs	*56* <0.1 Ba	*	*72* Hf	*73* <0.1 Ta	74 W	*75* <0.1 Re	*76* Os	*77* Ir	*78* Pt	*79* 0.26 2.1×10^{9} Au	*80* Hg	*81* Tl	*82* <0.1 Pb	*83* <0.1 Bi	*84* Po	*85* At	*86* Rn
87 Fr	*88* Ra	**	*104* Rf	*105* Db	*106* Sg	*107* Bh	*108* Hs	*109* Mt	*110* Ds	*111* Rg	*112* Cn	*113* Uut	*114* Fl	*115* Uup	*116* Lv	*117* Uus	*118* Uuo

- Impurity concentration kept below $5\times10^{10}/cm^2$.
- Better control of growth process and environment

ACS Applied Materials and Interfaces, 8 (39), 26400 (2016)

ICPMS Analysis of CVT WTe_2

1 H																	2 He
3 0.47 3.3×10^{8} Li	4 <0.1 Be			at. # ppbw at./cm^2 Element		$<1\times10^{10}/cm^2$	$>1\times10^{10}/cm^2$	Below detection limit	Not measured			5 <0.1 B	6 C	7 N	8 O	9 F	10 Ne
11 3.45 2.8×10^{9} Na	12 0.54 8.3×10^{8} Mg											13 0.2 4.6×10^{8} Al	14 Si	15 P	16 <50.00 S	17 Cl	18 Ar
19 0.68 1.3×10^{9} K	20 4.69 4.9×10^{9} Ca	21 <0.1 Sc	22 <0.1 Ti	23 0.15 5.8×10^{10} V	24 6.1 6.9×10^{9} Cr	25 0.18 6.9×10^{8} Mn	26 21.28 1.7×10^{10} Fe	27 2.78 4.5×10^{9} Co	28 2.58 4.2×10^{9} Ni	29 5.42 7.3×10^{9} Cu	30 <0.1 Zn	31 0.11 5.8×10^{8} Ga	32 <0.1 Ge	33 <0.1 As	34 <0.1 Se	35 Br	36 Kr
37 Rb	38 <0.1 Sr	39 Y	40 <0.1 Zr	41 0.15 8.6×10^{8} Nb	42 1.73 3.7×10^{9} Mo	43 Tc	44 <0.1 Ru	45 Rh	46 Pd	47 0.37 1.7×10^{9} Ag	48 <0.1 Cd	49 <0.1 In	50 0.14 9.7×10^{8} Sn	51 <0.1 Sb	52 Te	53 I	54 Xe
55 Cs	56 4.55 1.1×10^{10} Ba	*	72 Hf	73 <0.1 Ta	74 W	75 1.31 5.8×10^{9} Re	76 Os	77 Ir	78 Pt	79 4.26 1.3×10^{10} Au	80 Hg	81 TI	82 12.38 2.8×10^{10} Pb	83 <0.1 Bi	84 Po	85 At	86 Rn
87 Fr	88 Ra	**	104 Rf	105 Db	106 Sg	107 Bh	108 Hs	109 Mt	110 Ds	111 Rg	112 Cn	113 Uut	114 Fl	115 Uup	116 Lv	117 Uus	118 Uuo

- Impurity concentration kept below $5\times10^{10}/cm^2$.
- Better control of growth process and environment

Unpublished

Metrology Opportunities?

- Develop protocol for 2D materials impurity analysis
- Establish correlations with electronic/photonic device response

- Materials Challenges
- Methods
- TMDs
  - Defects
- Summary

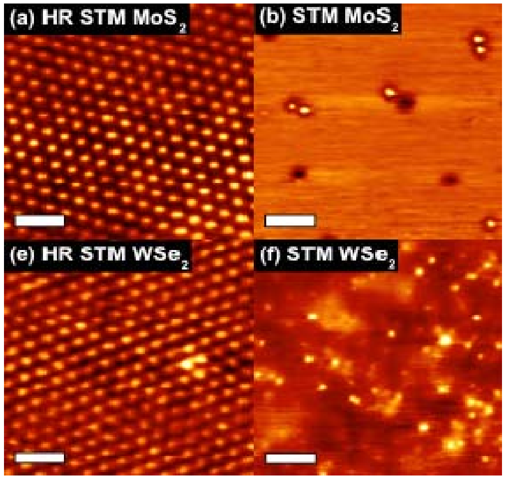

Exfoliated geological MoS_2

Reality!

- 100 nm × 100 nm

Pleasant to the “eye”!

- 13 nm × 13 nm

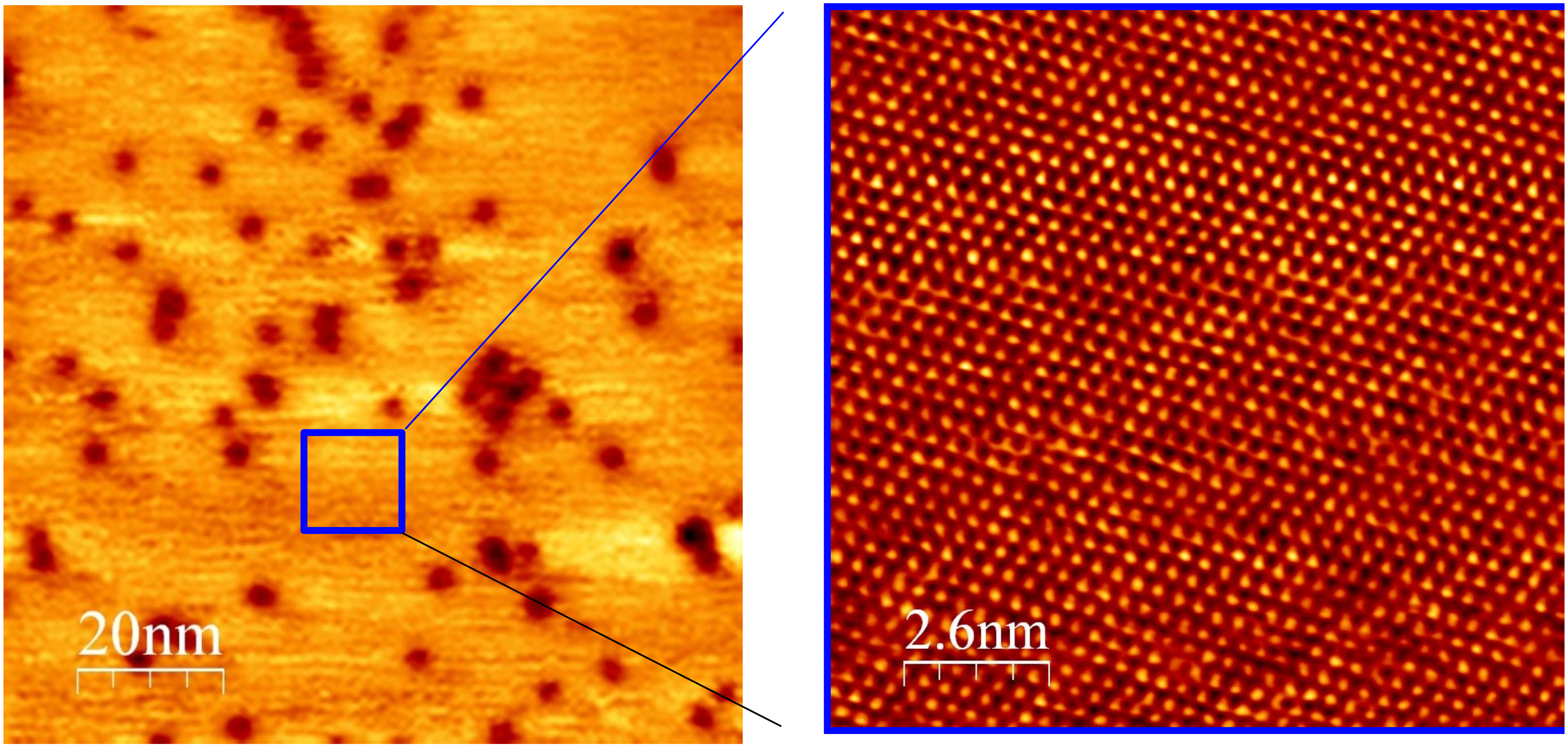

McDonnell, et al. *ACS Nano* 8, 2880 (2014)

More defect “Zoology” for Exfoliated MoS_2

Defects observed on exfoliated, geological MoS_2

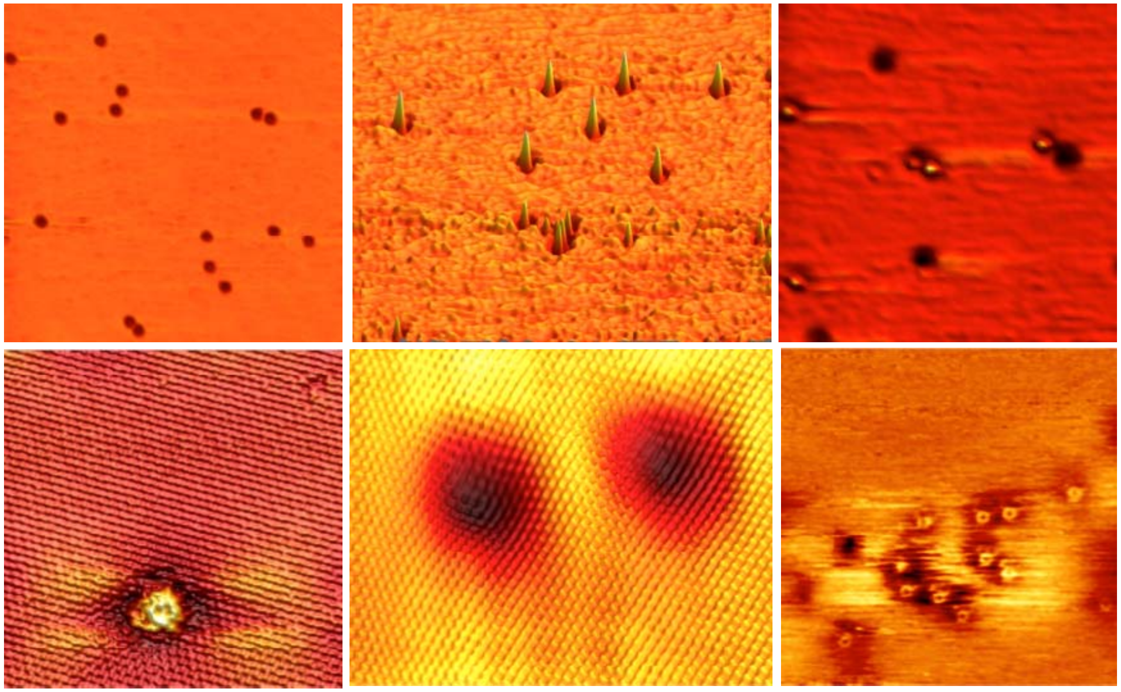

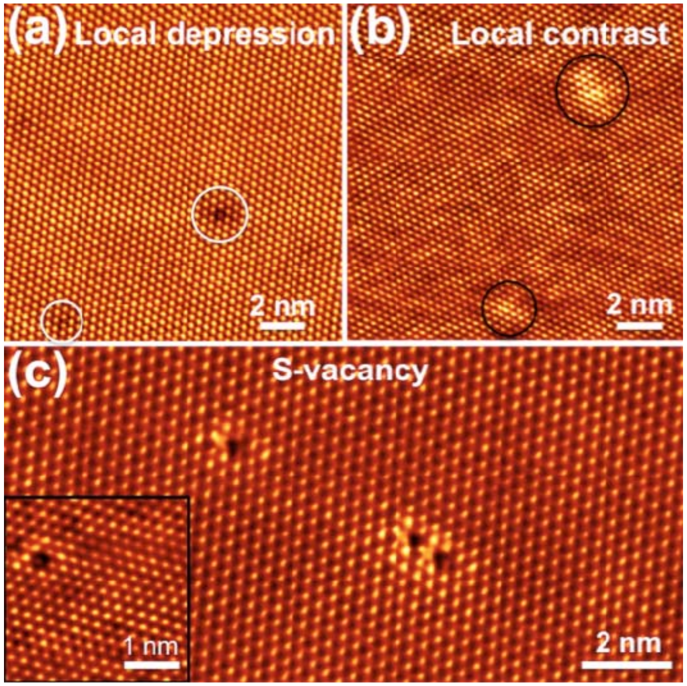

- Defect density up to 8 %.
- Various imperfections: metallic defects, donor and acceptor atoms, S-vacancy, structural defects…
- Impact on electronic and physical properties?

R. Addou, L. Colombo, R. M. Wallace. *ACS Appl. Mater. Interfaces* 7, 11921-11929 (2015)

Comparison of MoS_2 and WSe_2

Exfoliated TMDs

MoS_2

WSe_2

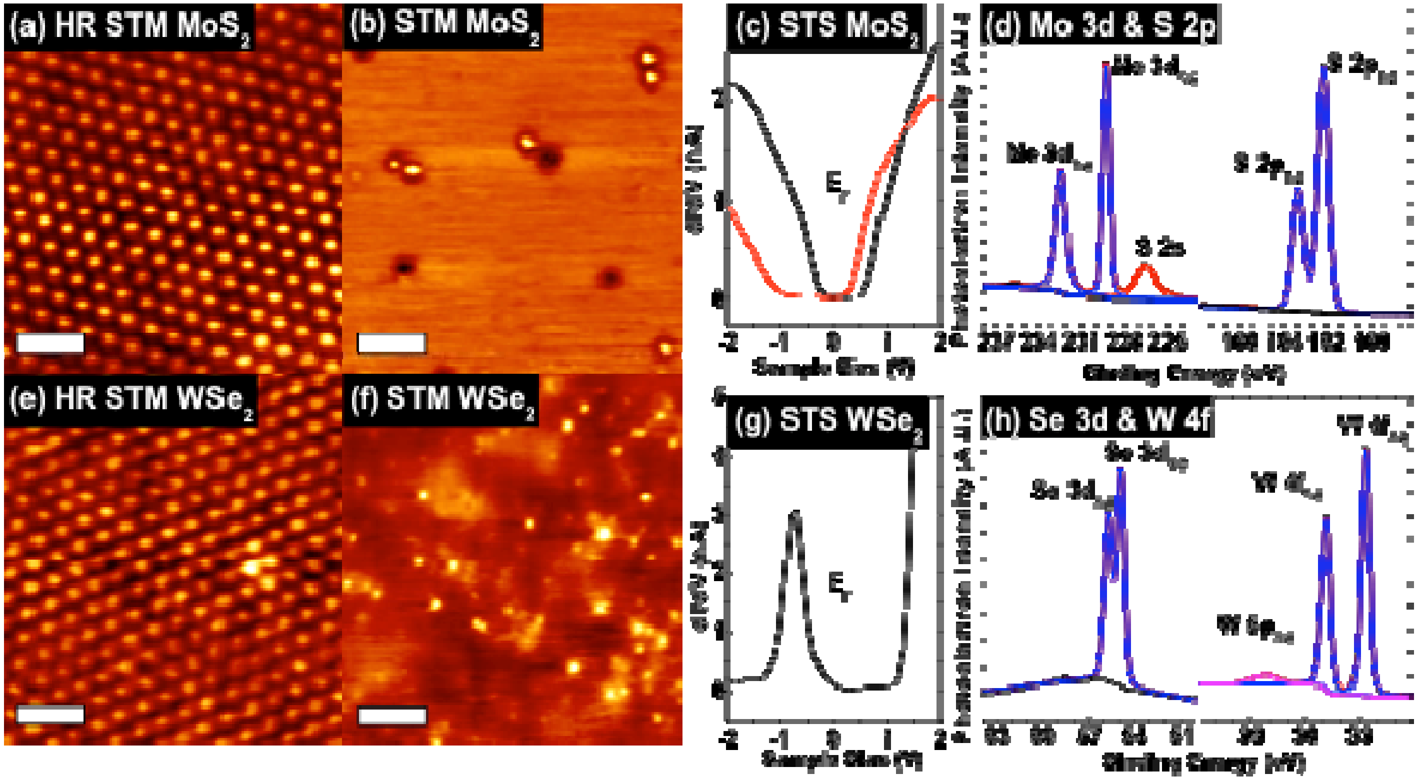

Figure 1. Initial MoS_2 (a−d) and WSe_2 (e−h) characterization. (a and e) High-resolution STM showing the atomic structure, scale bar 1 nm, imaging conditions (a) 0.7 V, 1 nA, and (e) 1.5 V, 1.5 nA. (b and f) 60 nm × 60 nm image showing that both surfaces are defective, scale bar 12 nm, imaging conditions (b) −0.3 V, 0.1 nA, and (f) 0.5 V, 1.3 nA. (c and g) STS spectra showing typical n- and p-type variability of MoS_2, and typically p-type behavior of WSe_2. (d and h) XPS of the initial surfaces showing the expected MoS_2 and WSe_2 chemical states.

- Defects evident at the atomic scale
- STS shows defect impact on doping

ACS Nano, 8, 6265 (2014)

Variations in Exfoliated WSe$_2$

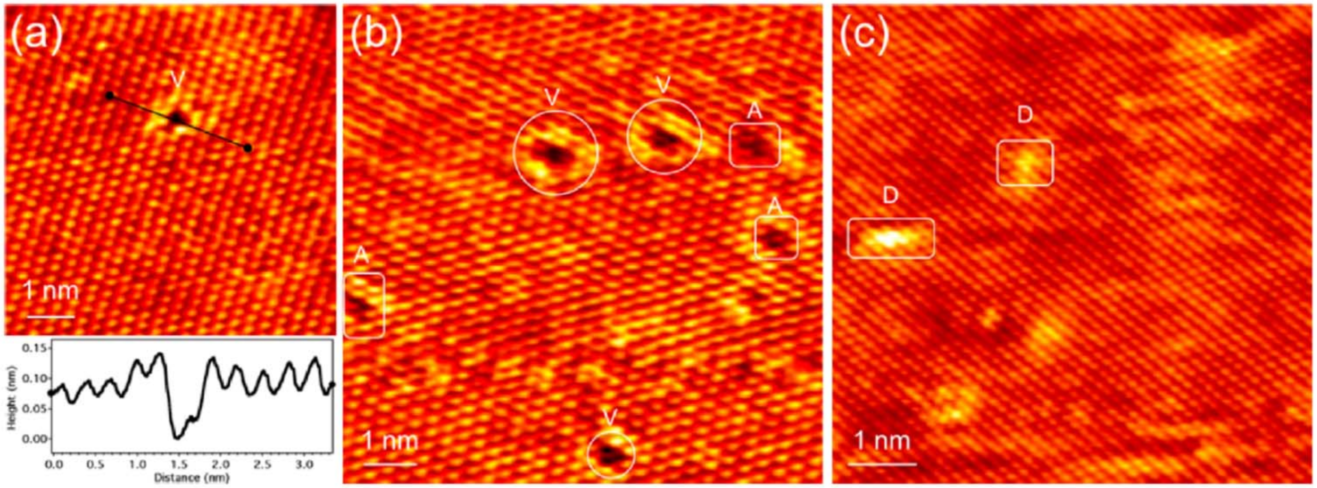

Figure 2. Imaging of atomic size imperfections on WSe$_2$ (sample A). (a) STM image (V_b = 1.5 V, I_t = 1.5 nA) shows a single Se vacancy with the corresponding line profile. (b) STM image (V_b = 1.5 V, I_t = 1.5 nA) showing two types of point defects: single vacancy (noted as "V") and local depression (noted as "A") caused by the presence of an acceptor at this area. (c) STM image (V_b = 1.5 V, I_t = 0.5 nA) shows an atomic bright spot (noted as "D") induced by the presence of donor atom at the vicinity of the surface.

- Defects evident at the atomic scale
  - "V" type density: ~0.7×10^{12}/cm^2
  - "D" type density: ~1.7×10^{12}/cm^2
  - "A" type density: ~1.2×10^{12}/cm^2

ACS Appl. Mat. Int. 8, 6265 (2014)

Variations in Exfoliated WSe_2

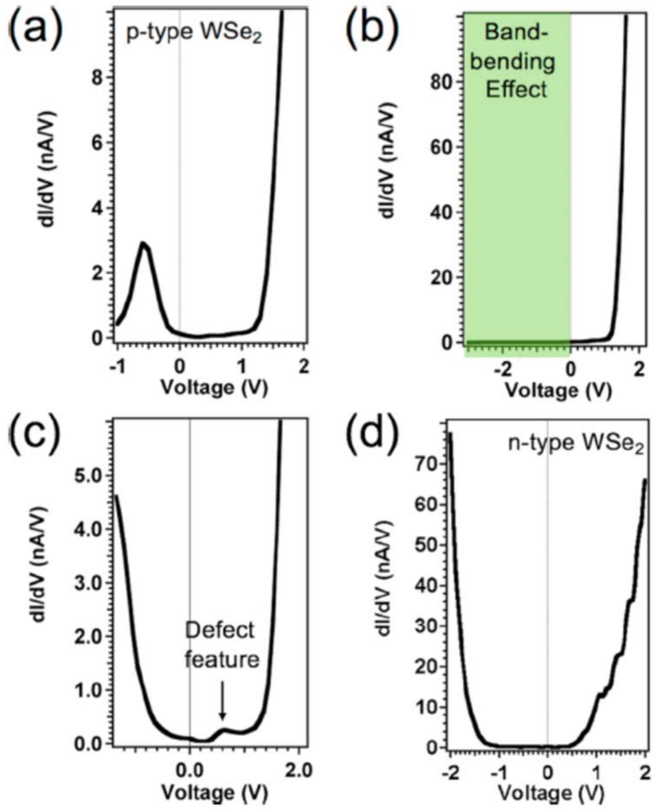

Figure 3. dI/dV vs V spectra recorded on two different freshly exfoliated WSe_2 samples (A, B) showing different behaviors: (a) p-type conductivity, (b) band bending effect ($I_t \sim 0$ when $V_b = 0$), (c) defect state in the gap, and n-type conductivity.. The STS in (a−c) was recorded on sample “A”, and the STS in (d) was recorded on sample “B”.

- Electronic structure variation
  - P-type
  - N-type
  - Gap states
  - Tip/Band bending effects?

ACS Appl. Mat. Int. 8, 6265 (2014)

Variability of Contacts on bulk, exfoliated MoS_2

- Noticeable variations in the core-level spectra are observed across an MoS_2 sample
- Low binding energy shoulder on the Mo 3*d*
- Degree of variability is vendor material specific
- Highest quality vendor materials can still result in ~20% of the surface exhibiting regions with shoulder features

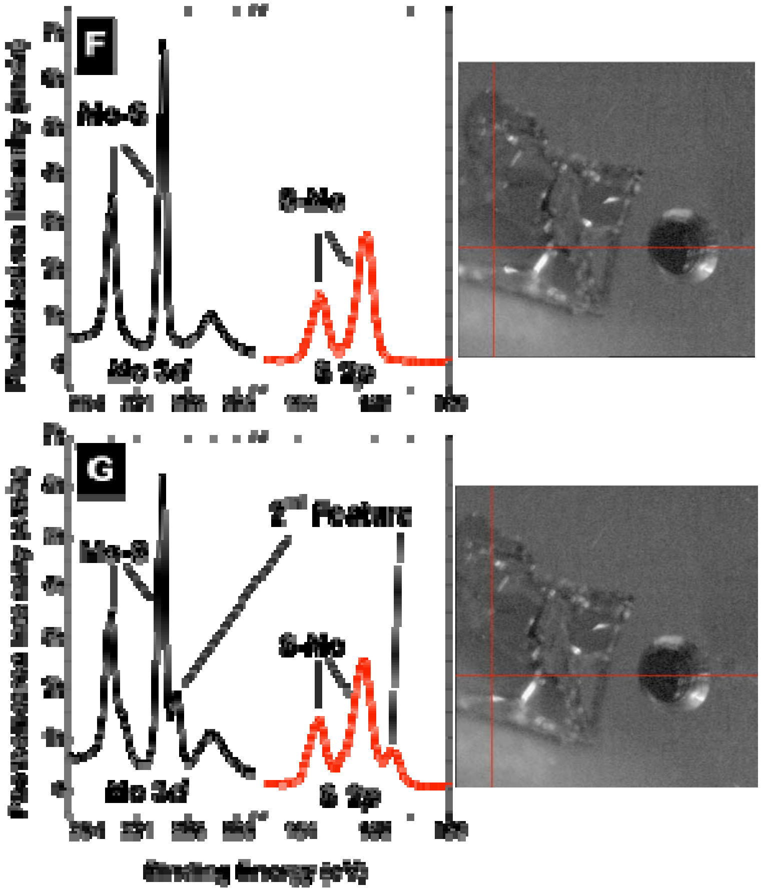

XPS variability

McDonnell, et al. *ACS Nano* 8, 2880 (2014)

UT DALLAS

Correlating I-V measurements with STM, STS and XPS: MoS_2

- All the measurements are performed on the identical spot
- Reproducible regardless of the order of measurements

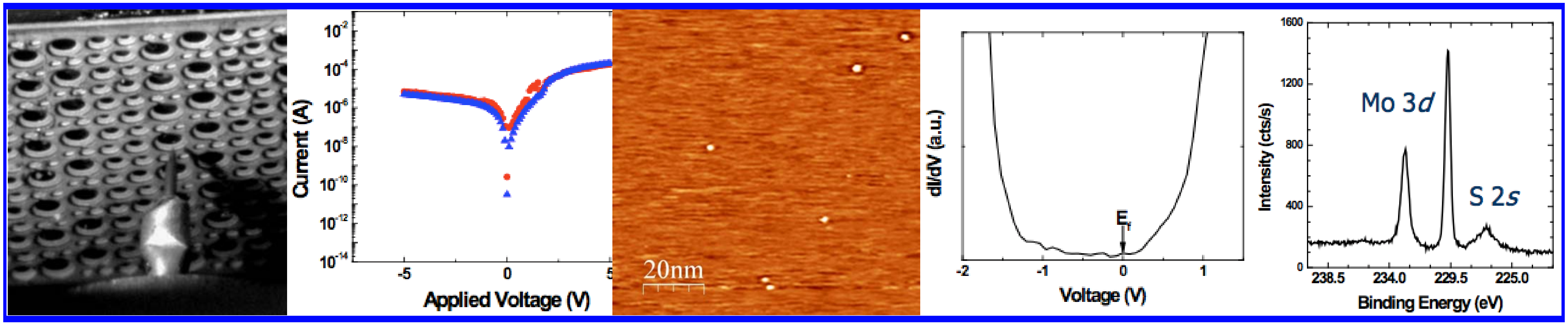

At ~1.25 mm far away:

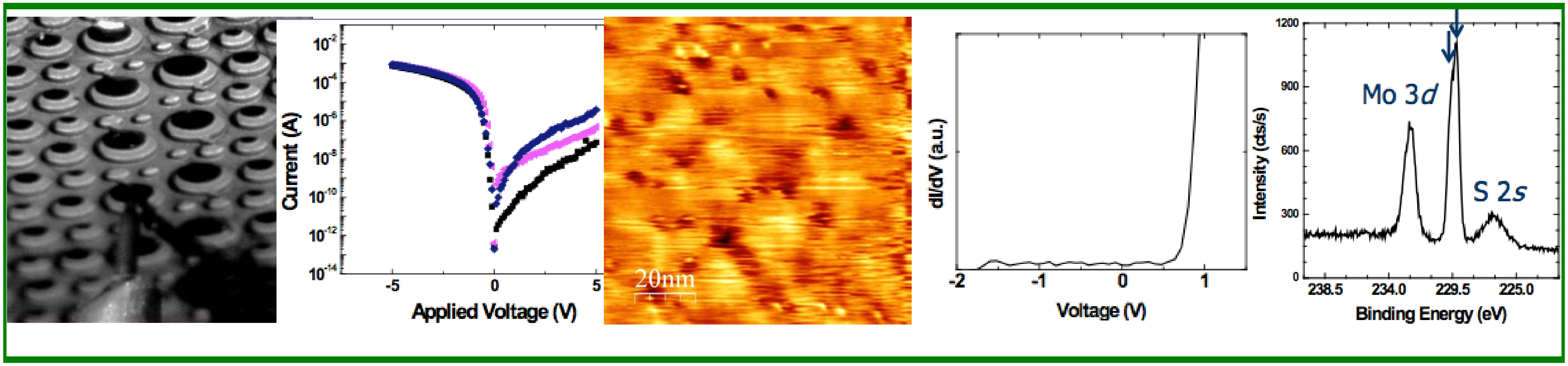

- **Correlation founded between defects and the level of variability**
  - **Regions with low defect density – n-type MoS_2 (S:Mo = 1.8:1)**
  - **Regions with high defect density – p-type MoS_2 (S:Mo = 2.3:1)**

McDonnell, et al. *ACS Nano* 8, 2880 (2014)

Metrology Opportunities?

- Develop protocol for 2D materials defect analysis and densities

- Establish correlations with electronic/photonic device response (D_{it}, lifetime, etc)

- Materials Challenges
- Methods
- TMDs
  - Contacts
- Summary

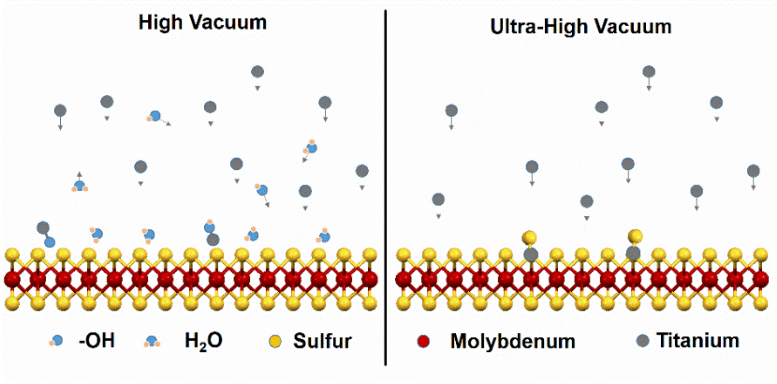

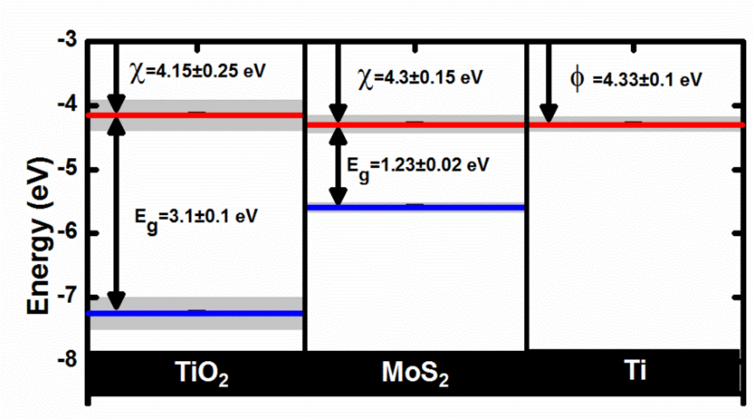

Cr Contacts Deposited in HV vs. UHV

UHV System

P~10^{-9} mbar

Few-layer MoS_2 exfoliated by scotch tape and transferred to Si wafer with 270 nm SiO_2

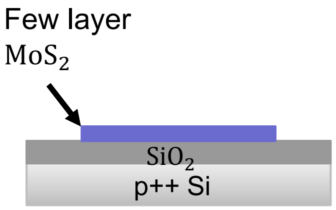

Metal deposition for **S/D** contacts and lift-off

Cleanroom Cryo Evap P~10^{-6} mbar

One device had Au/Cr S/D deposited in **UHV** and other device in the **Cleanroom HV**

UHV Anneal at 300 °C for interface cleaning

In-situ UV-O_3 treatment and high-k deposition

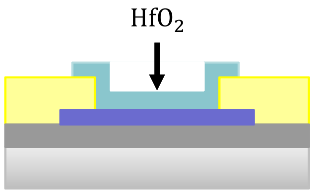

Gate patterning, Au/Cr deposition and lift-off

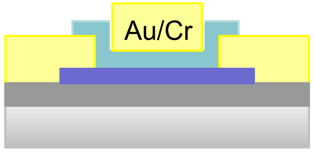

Both devices had their Au/Cr **top gate** deposited in the Cleanroom

Submitted, with C. Young

UT DALLAS

Cr Contacts Deposited in HV vs. UHV

HV (Cleanroom) & UHV Comparison

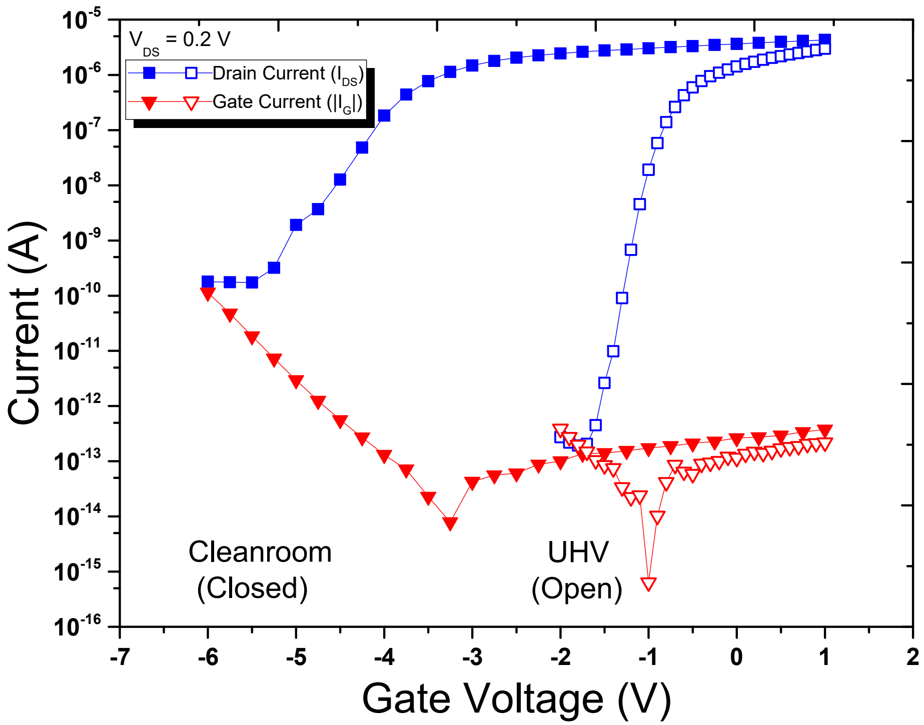

UHV I_D-V_D

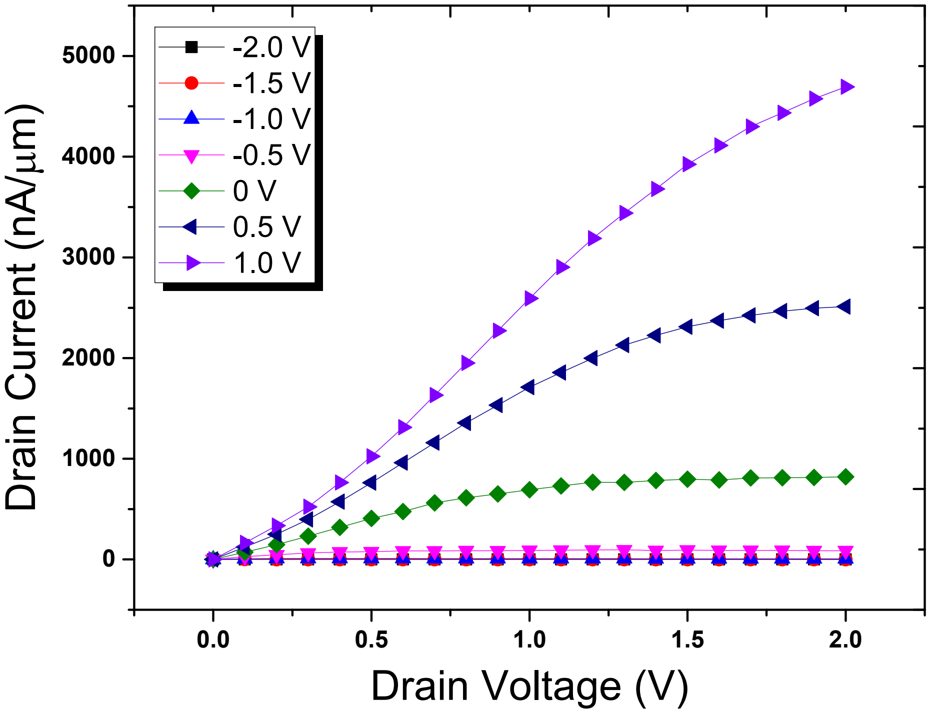

- Lower threshold voltage
- Increase in on/off ratio
- Reduction in contact resistance

Submitted, with C. Young

Cr Contacts Deposited in HV vs. UHV

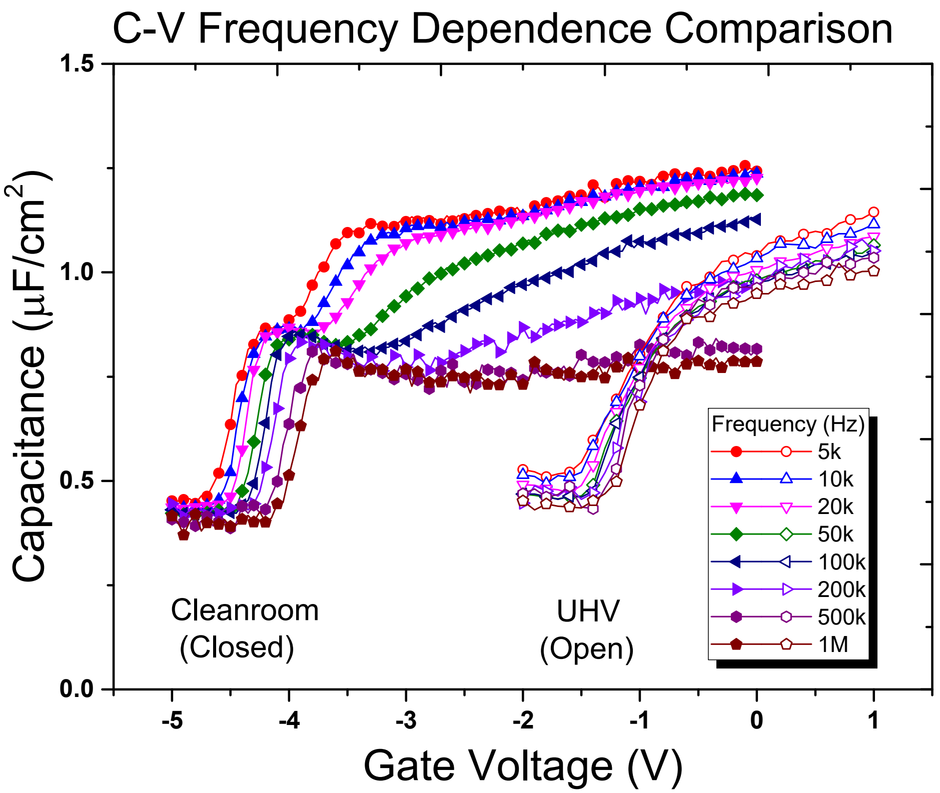

- Less dispersion over a large frequency range is due to lower series resistance
- Lack of "humps" in the depletion of UHV sample suggests a smaller number of interface traps

Submitted, with C. Young

HV vs. UHV Contact Metal Deposition

- Comparison of cleanroom tool (HV) and UHV deposition ambient reveals significant differences in contact interfacial chemistry for MoS_2…

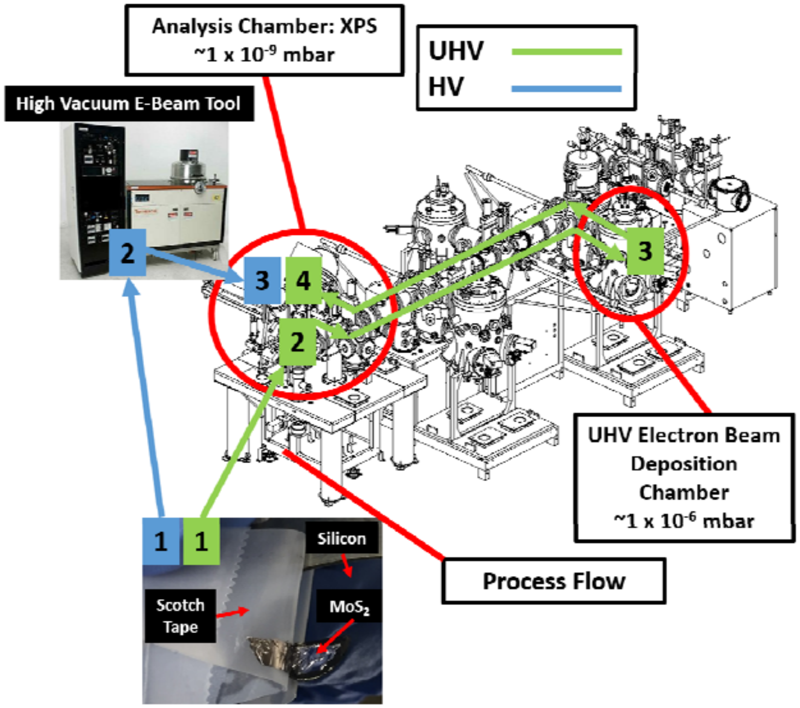

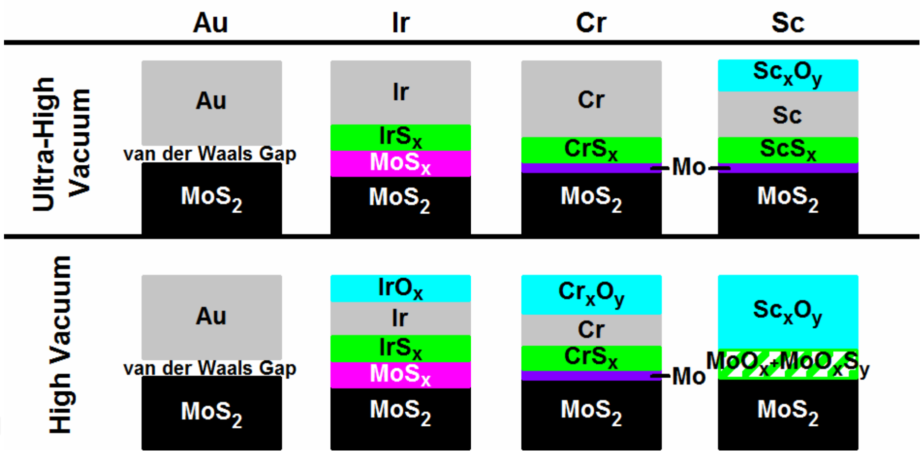

Ti/MoS_2*: See ACS Applied Materials and Interfaces*, **8** (12), 8289–8294 (2016)

C. Smyth, et al., *J.Phys.Chem*. C **120** (27), 14719 (2016)

MoS_2/Cr interface

- Deposition by cleanroom tool (HV)
  - CrO_x formation detected
  - Some CrS_x reaction products also detected
- UHV deposition ambient reveals
  - CrO_x formation below limit of detection
  - More CrS_x formation detected
- Interfacial chemistry very different depending upon deposition process ambient
- UHV ambient appears to correlate with improved device behavior

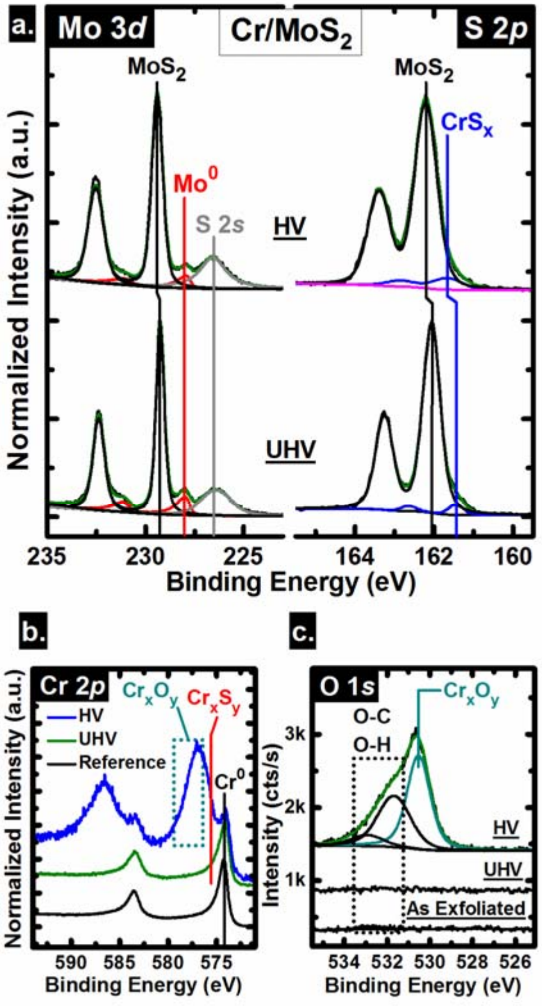

C. Smyth, et al., *J.Phys.Chem*. C **120** (27), 14719 (2016)

Contact Metal Interfacial Chemistry

Au

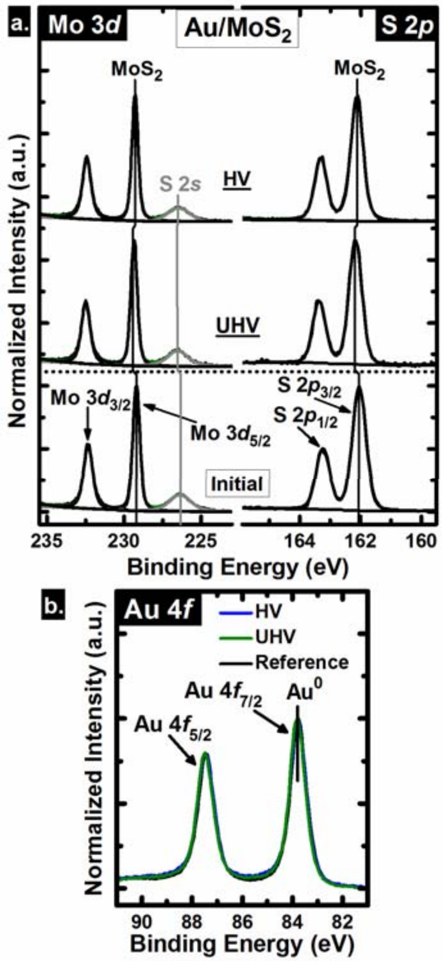

Ir

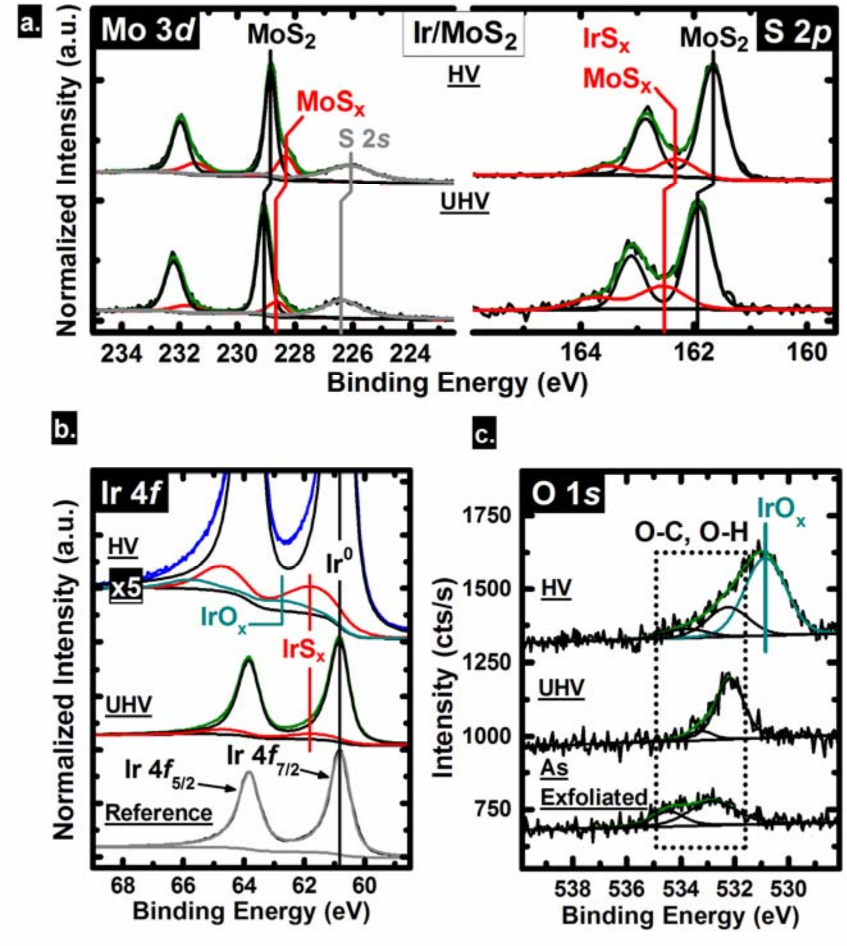

- No reaction of Au with the MoS$_2$ substrate detected
- Oxygen species (HV) can partially mitigate the reaction with Ir

C. Smyth, et al., *J.Phys.Chem*. C **120** (27), 14719 (2016)

Contact Metal Interfacial Chemistry

Comparison of contact interfaces from cleanroom (HV) vs. UHV deposition

Cr

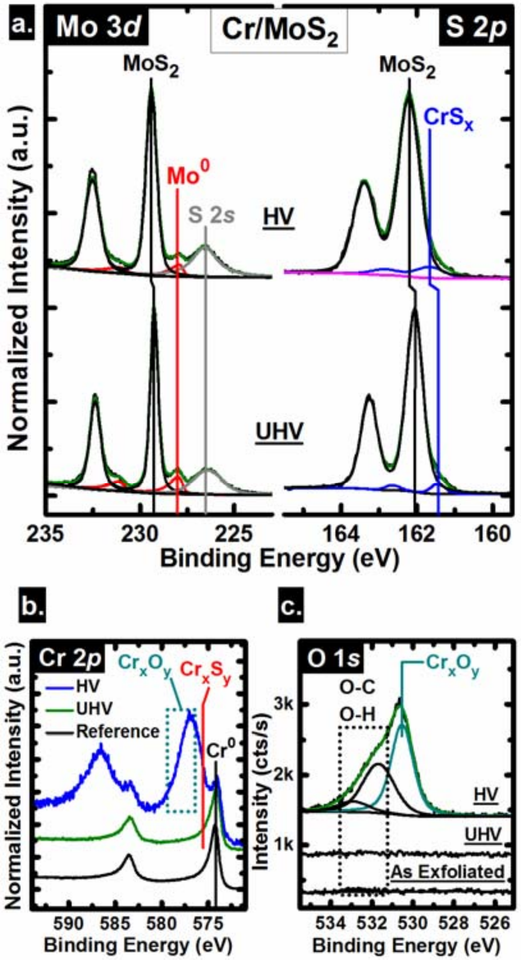

Sc

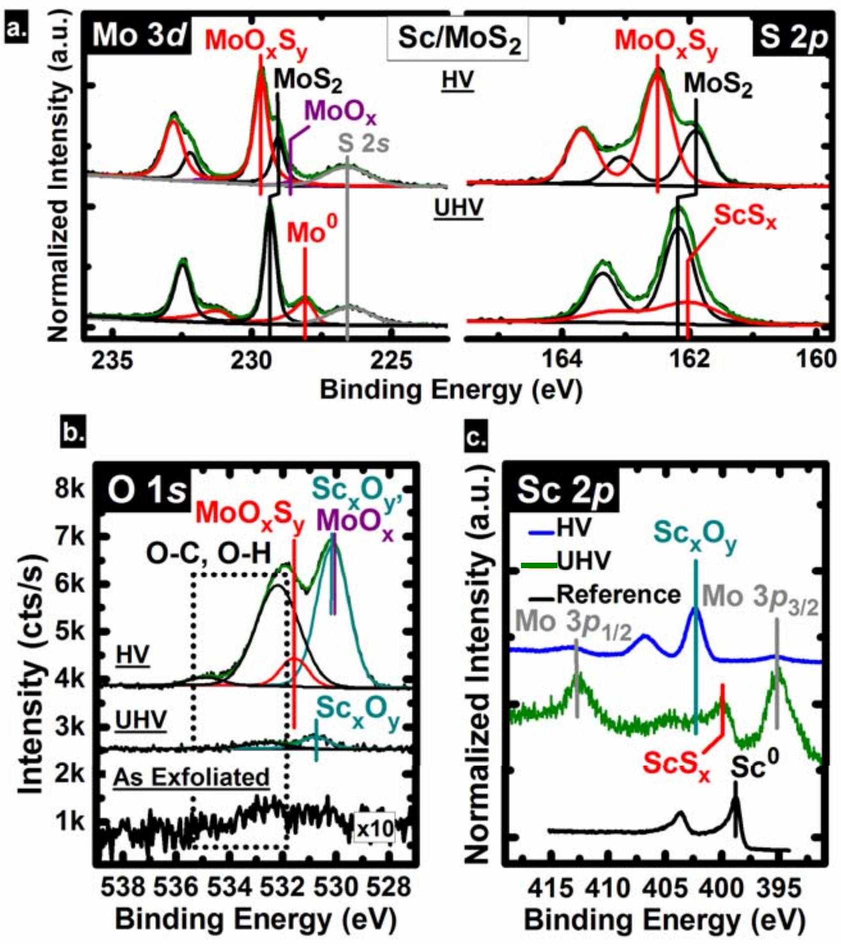

- Both Cr and Sc react with the MoS_2 substrate
- Oxygen species (HV) can Partially mitigate the reaction

C. Smyth, et al., *J.Phys.Chem.* C **120** (27), 14719 (2016)

HV vs. UHV Contact Metal Deposition

- Comparison of cleanroom tool (HV) and UHV deposition ambient reveals significant differences in contact interfacial chemistry for MoS_2…

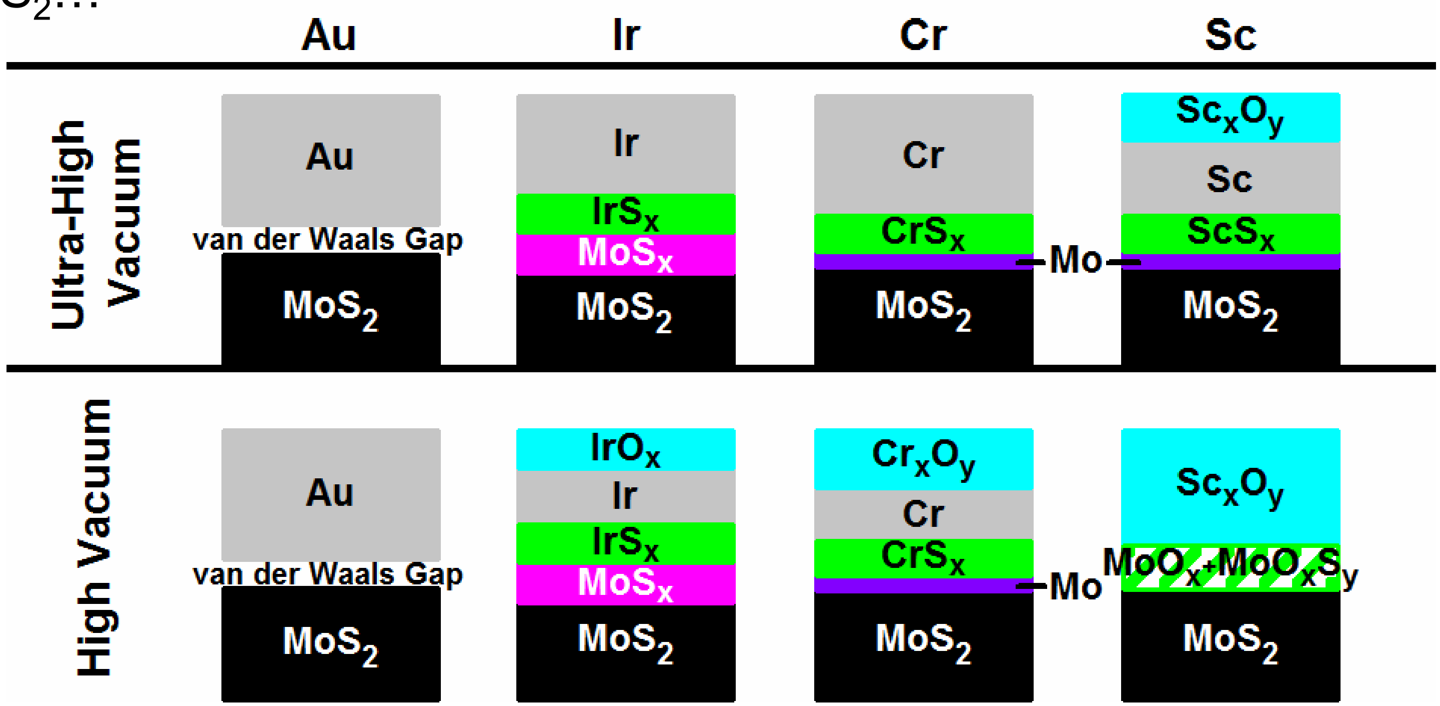

Ti/MoS_2: See also *ACS Applied Materials and Interfaces*, **8** (12), 8289–8294 (2016)

Pop group recent work, Nanoletters (2016)
http://dx.doi.org/10.1021/acs.nanolett.6b01309

C. Smyth, et al., *J.Phys.Chem*. C **120** (27), 14719 (2016)

Metrology Opportunities?

- Develop protocol for 2D materials contact characterization (physical and electrical)

- Establish correlations with electronic/photonic device response

- Materials Challenges
- Methods
- TMDs
  - Functionalization
- Summary

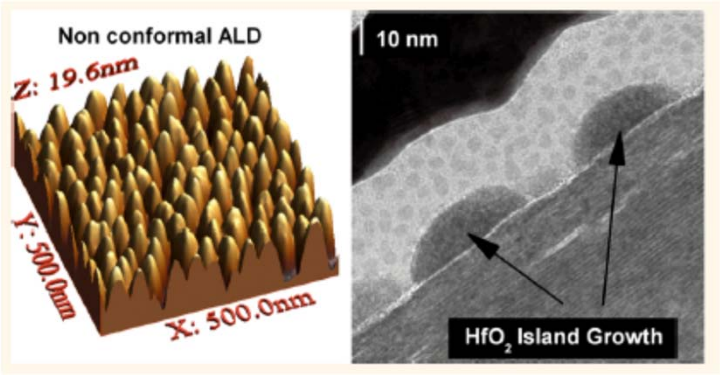

High-k/2D Interfaces

- Transition metal dichalcogenides (TMDs) based transistor has drawn significant attention because of the two dimensional structure and moderate bandgap value (1.8 – 1.2eV).

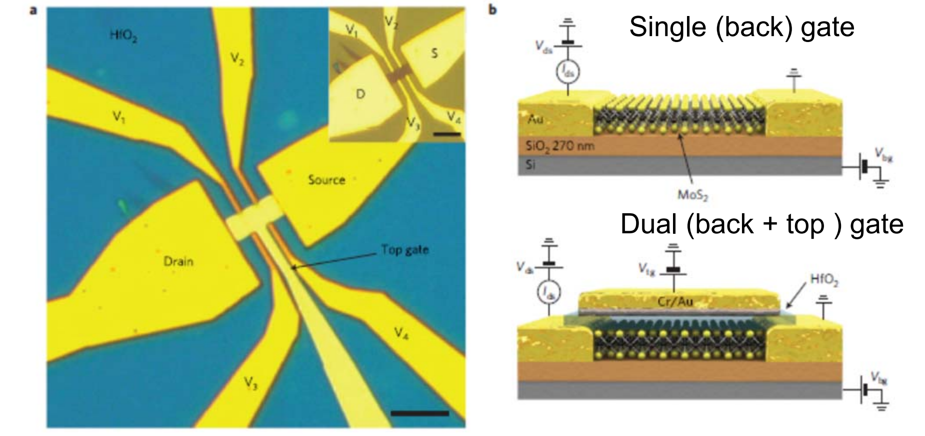

Figure 1 | Fabrication of single-gated and dual-gated MoS$_2$ devices. a, Optical image of the MoS$_2$ dual-gated device used in our measurements. The inset shows the single-gate version of the same device before ALD deposition of HfO$_2$ and top-gate electrode fabrication. Scale bars, 5 µm. **b**, Cross-sectional views of devices based on single-layer MoS$_2$ in a single-gate (top) and dual-gate (bottom) configuration. Gold leads are used for the source, drain and voltage probes (V$_1$, V$_2$, V$_3$ and V$_4$). Voltage probes have been omitted from the drawing. The silicon substrate, covered with a 270-nm-thick SiO$_2$ layer was used as the back gate. The top-gate dielectric is a 30-nm-thick HfO$_2$ layer.

Radisavljevic and Kis, Nat. Mat. 12 (2013) 815

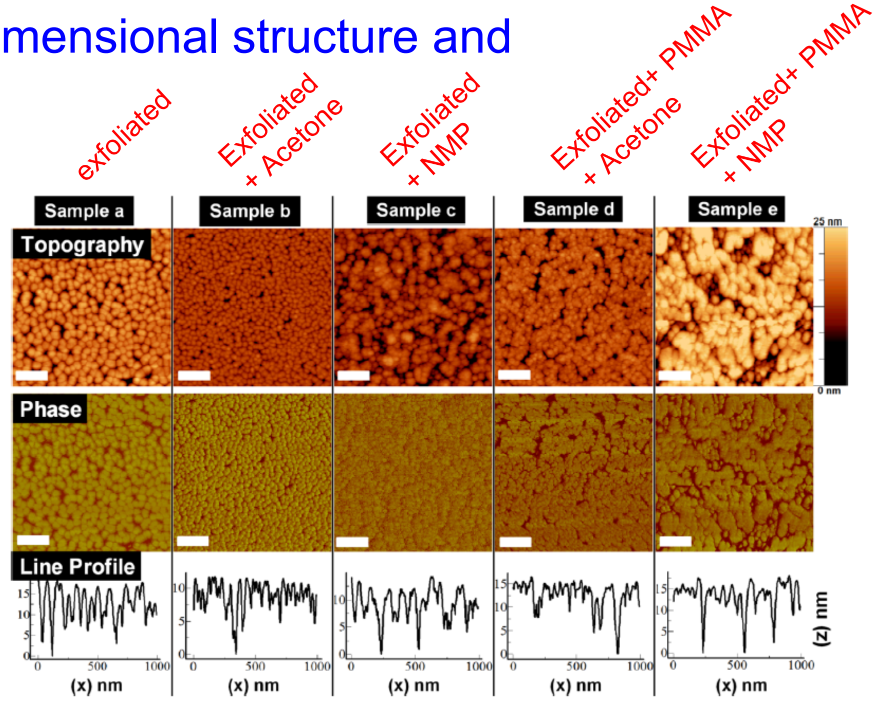

AFM images of ALD HfO$_2$ on MoS$_2$ *without* surface functionalization (only residues!)

- Due to the relatively inert surface of sulfide-based TMDs, deposition of high-k dielectrics and surface functionalization on TMDs have been investigated.

S. McDonnell, et al., *ACS Nano.* **7** (2013) 10354; A. Azcatl, et al., *Appl. Phys. Lett*. **104** (2014) 11160; A.Azcatl, et al., *2D Materials* **2** (2015) 014004; P.Zhao, et al., *Microeletronic Eng.* **147** (2015) 154

Functionalization by UV-O_3 - Apparatus

Sample surface (facing down) is <3mm from lamp

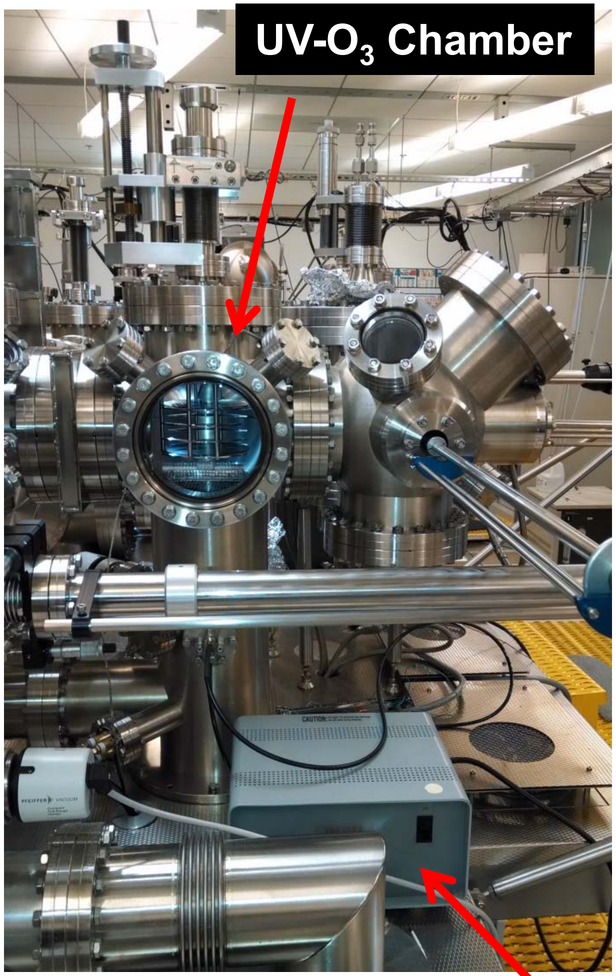

UV-O_3 Chamber

UV-Lamp Power Supply

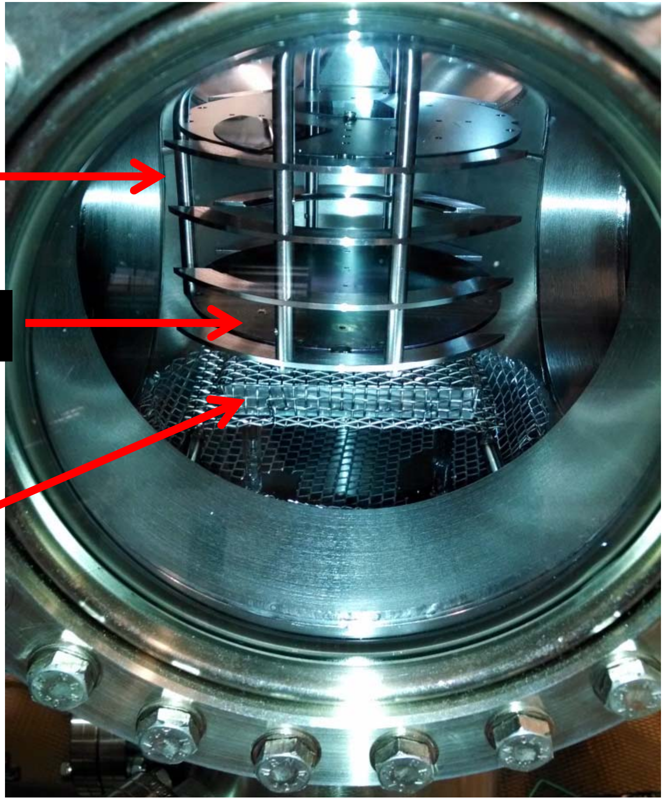

UV-O_3 Chamber

Carousel

Sample Plate

UV-Lamp with protective mesh

UT DALLAS

Cleaning up MoS_2...In-situ analysis

- C contamination reduced below detection limit
- S-O bonding formation: functionalization
- Mo-O bonding not detected

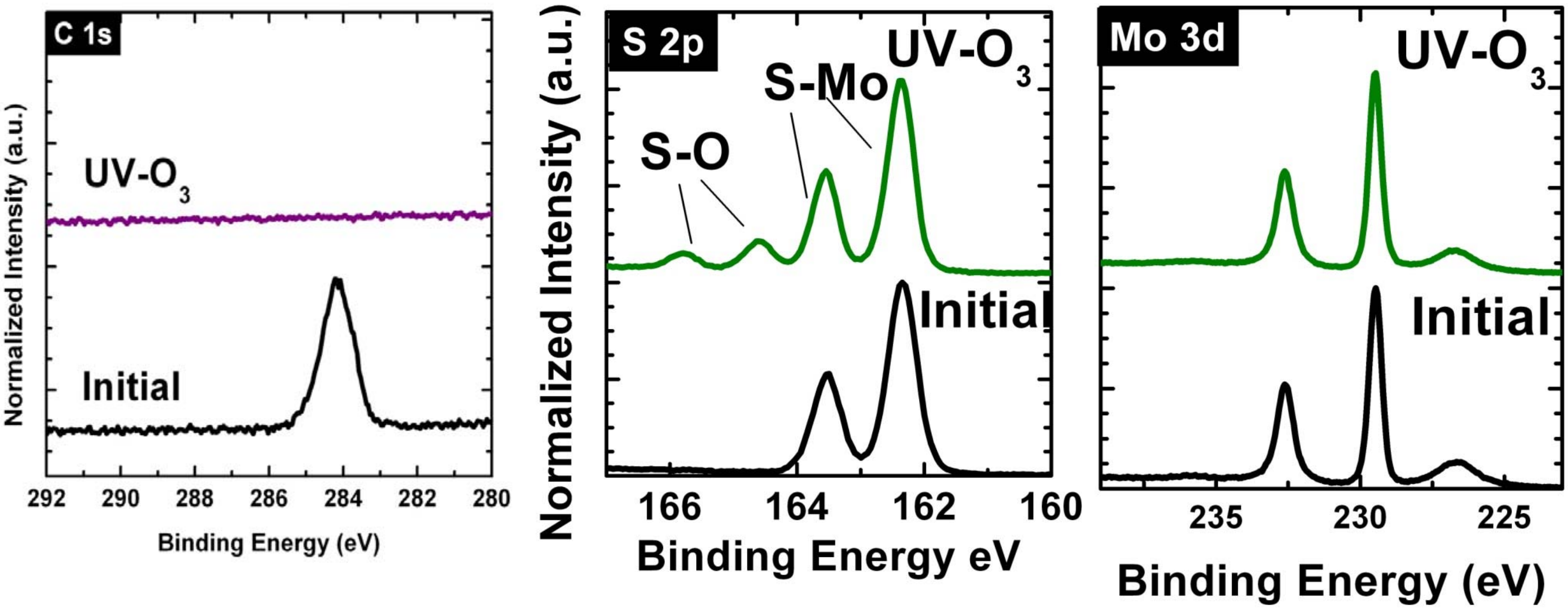

A. Azcatl, et al., *APL* 104, 111601 (2014)

Improved uniformity for Al_2O_3

ALD: 200°C, TMA-H_2O

ALD only

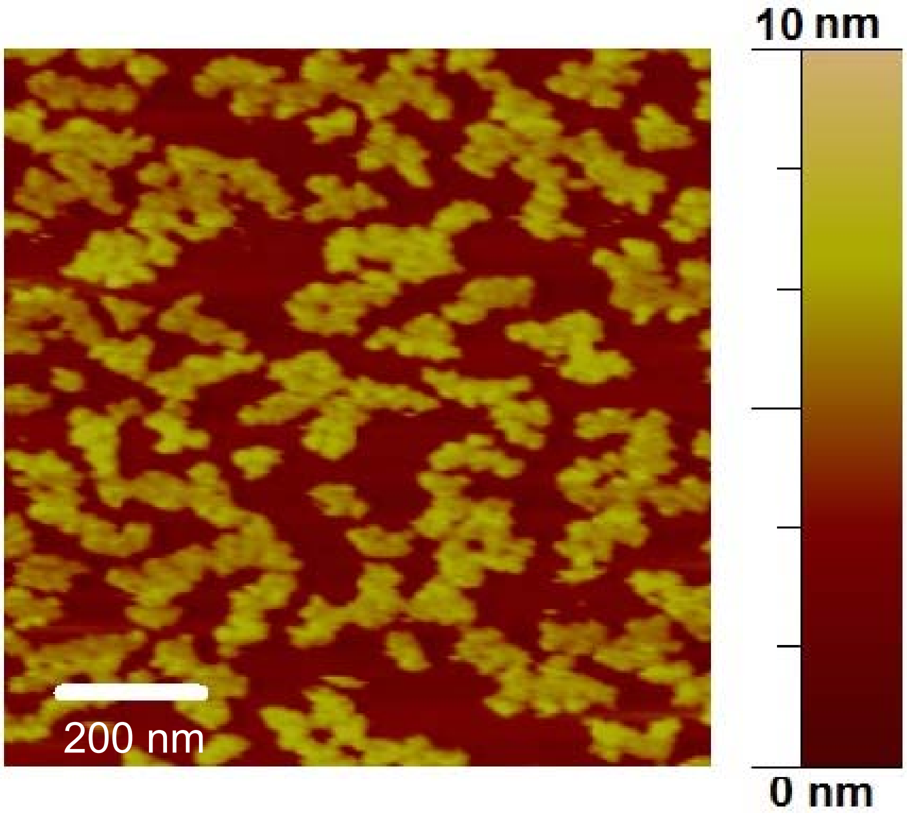

Surface Preparation: Exfoliation

UV-O_3 + ALD

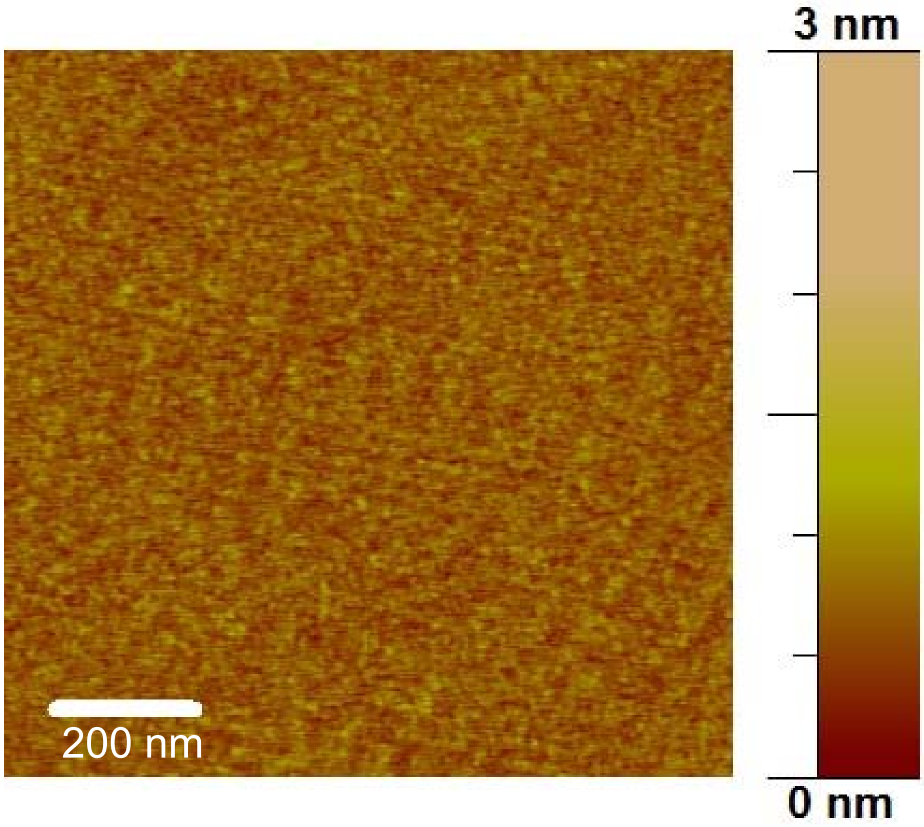

900 mbar O_2, 15 minutes, room temperature

A. Azcatl, et al., *APL* 104, 111601 (2014)

UT DALLAS

Top-gate MoS_2-based FETs: Electrical Characterization

In collaboration with Prof. Chadwin Young, Prof. Paul Hurley, and Mr. Peng Zhao

Device Structure

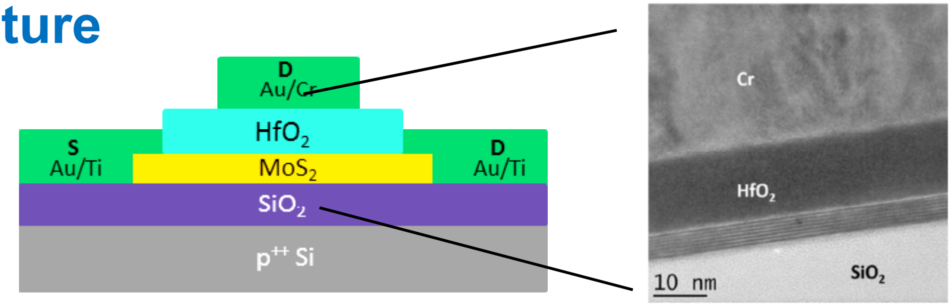

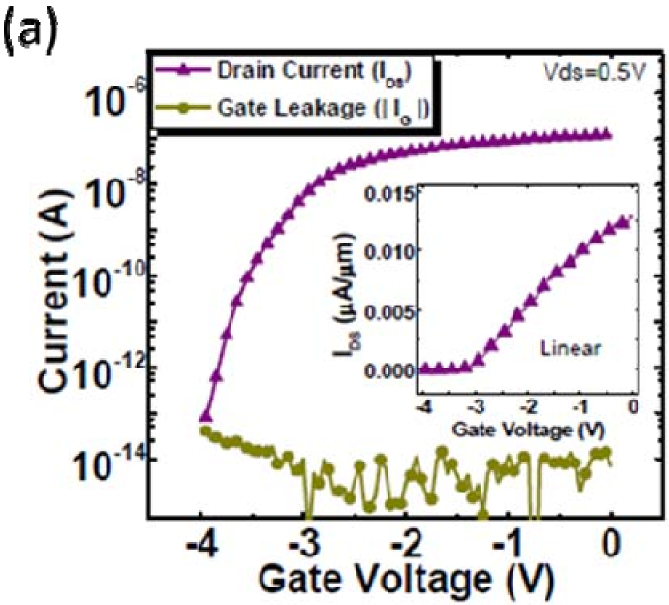

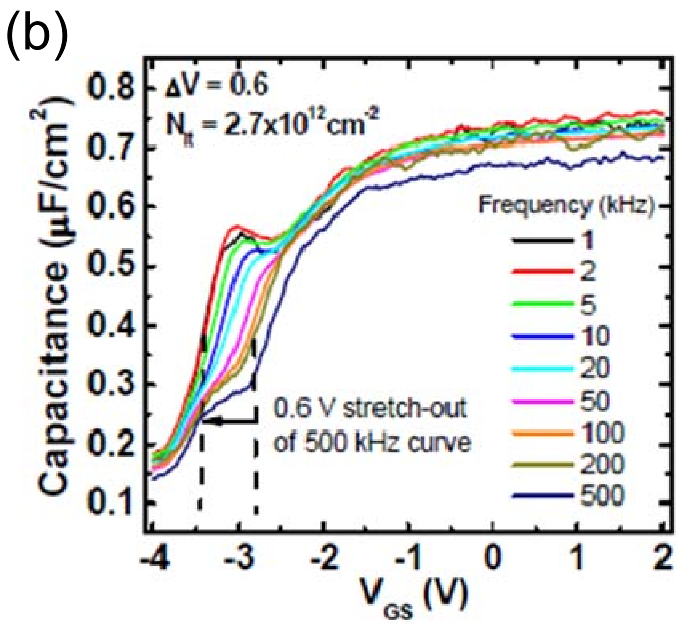

- High I_{ON}/I_{OFF} ratio $\sim 10^6$
- Low leakage current level $\sim 10^{-14}$ A → Good insulating properties of HfO_2

- Hump → Interface trap charge response
- **$D_{it} \approx 2.7\times10^{12}$ cm^{-2}**

Zhao, P., *et al*. 2016, submitted.

Metrology Opportunities?

- Develop protocol for 2D materials cleaning, controlled functionalization, characterization (physical and electrical)

- Establish correlations with electronic/photonic device response

- Materials Challenges
- Methods
- TMDs
    - Doping
- Summary

UT DALLAS

Nitrogen doping of MoS_2 by remote N_2 plasma exposure

*In-situ XPS

Covalent Nitrogen doping of MoS_2

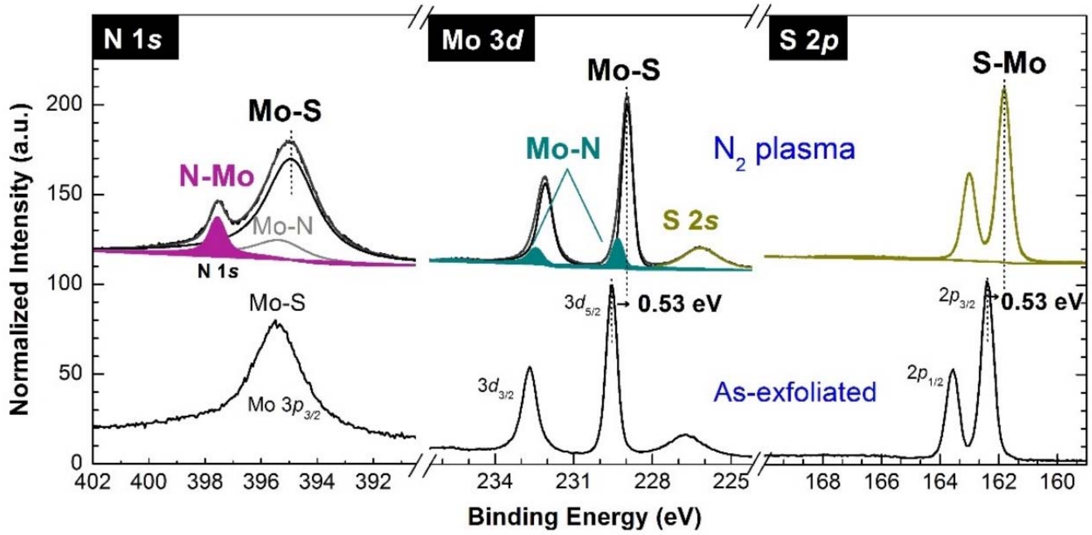

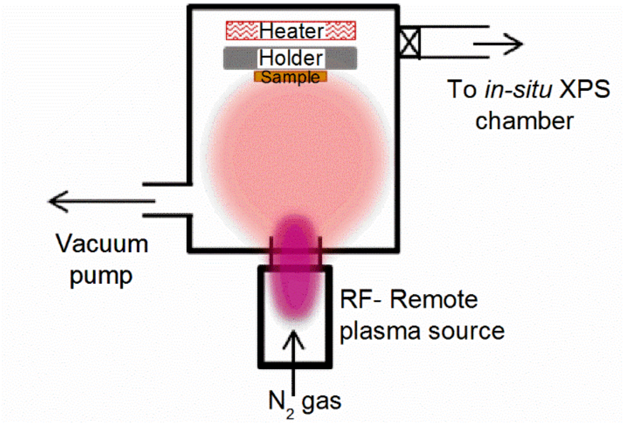

Sulfur substitution by Nitrogen

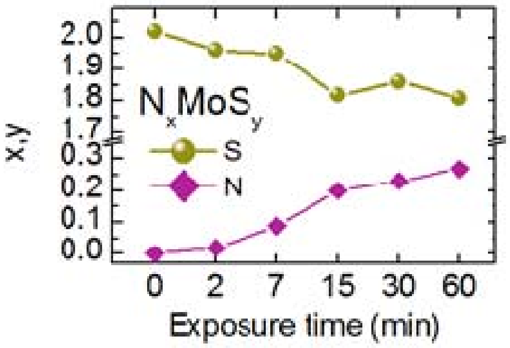

Controllable at% Nitrogen

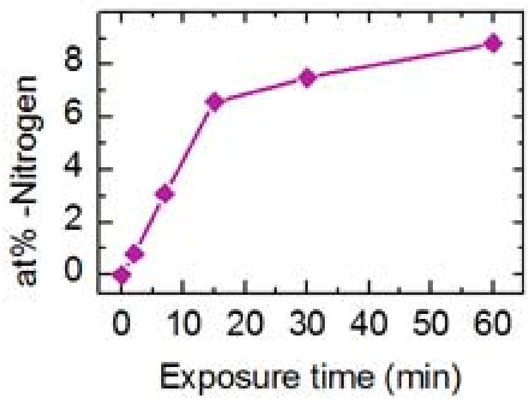

- *Nitrogen concentration controlled with N_2 plasma exposure time*

Azcatl, et al. *Nanoletters* **16** (9), 5437 (2016)

Nitrogen doping of MoS_2 by remote N_2 plasma exposure

Strain induced by Nitrogen doping in MoS_2

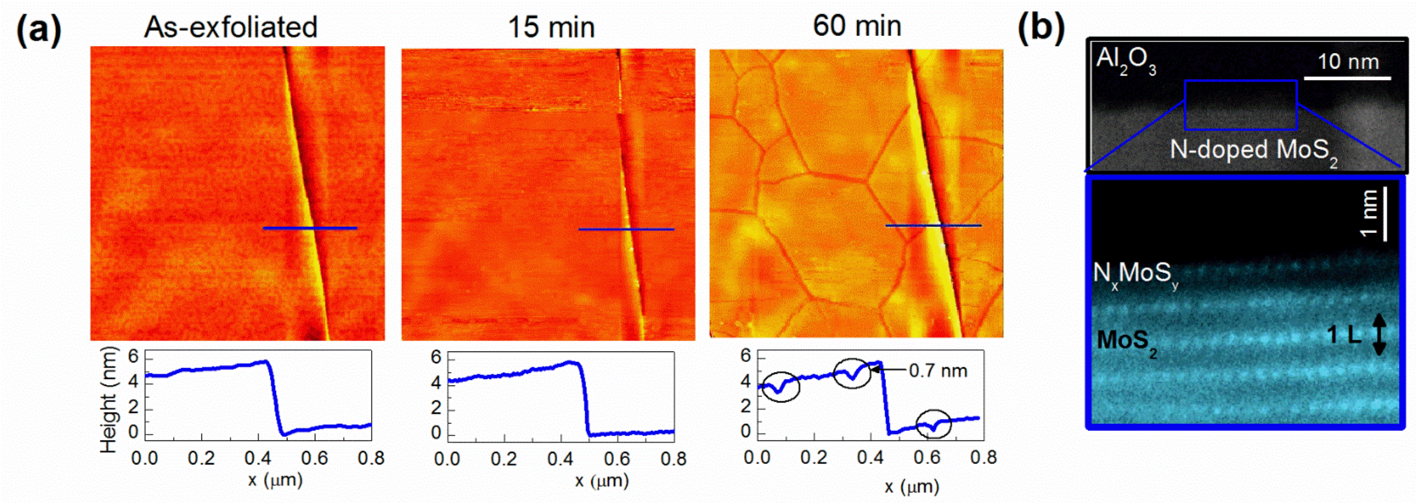

- Compressive strain was identified in MoS_2 - Blue shift of both E^1_{2g} and A_{1g} Raman modes[1]
- Compressive strain can be tuned with nitrogen coverage up to 1.7% at 1 ML

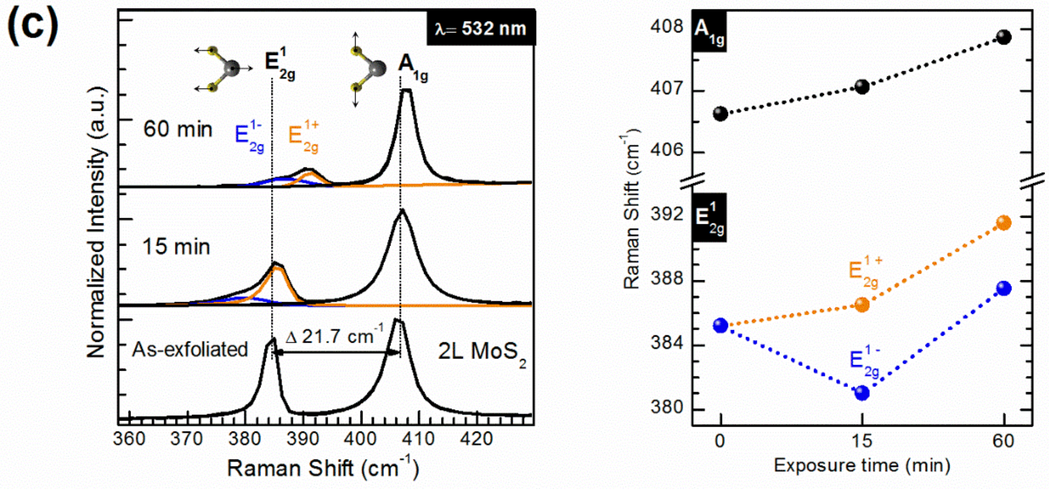

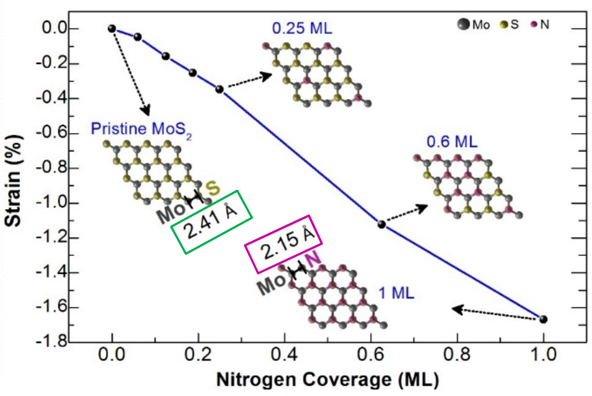

Azcatl, et al. *Nanoletters* **16** (9), 5437 (2016)

P-TYPE DOPING OF MOS_2 ENABLED BY NITROGEN DOPING

Electrical Characterization of Nitrogen Doped MoS_2

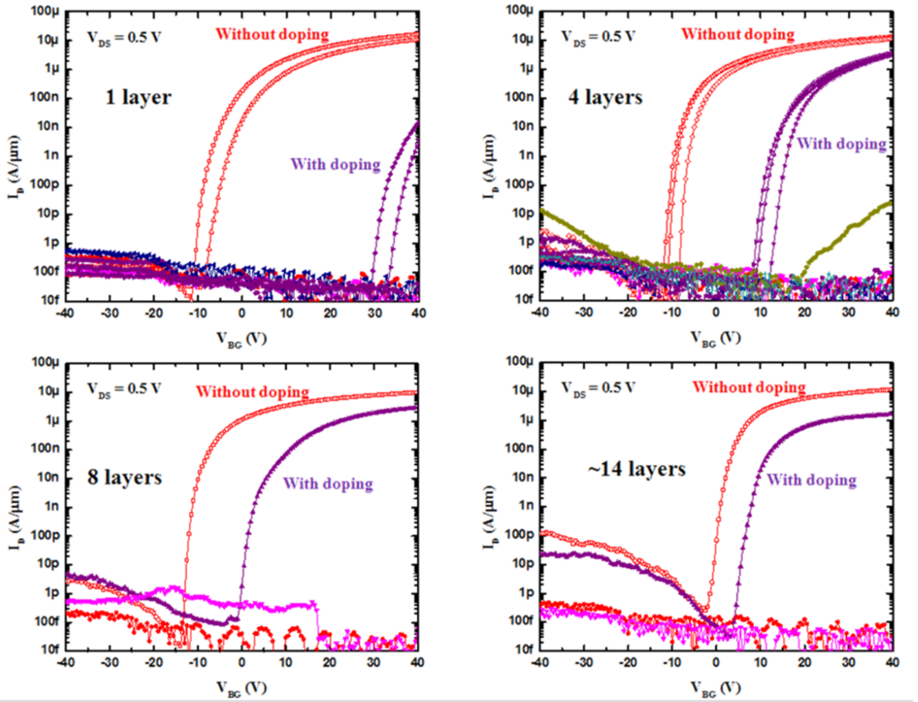

Nitrogen doped MoS_2 Stoichiometry: $N_{0.2}MoS_{0.8}$

- ✓ **Threshold voltage shift consistent with the claim of p-doping**
- ✓ **ON current levels are preserved**

Device Structure

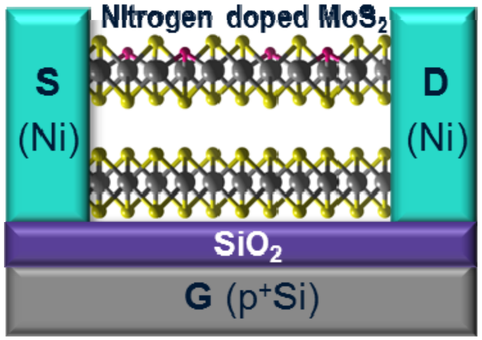

Channel Thickness Dependent Shift

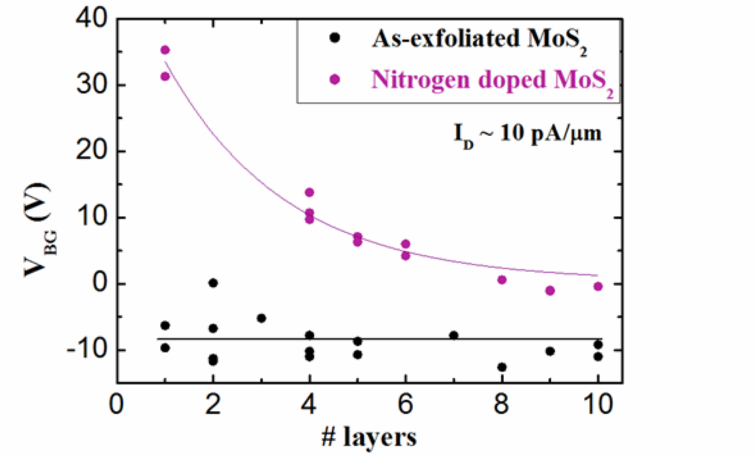

- ✓ **The donor doping level in Nitrogen doped MoS_2 was found to be in the range of ~ 2.5×10^{18} cm^{-3} - 1.5×10^{19} cm^{-3}, having a reference doping level of 1.55×10^{18} cm^{-3} for undoped MoS_2**

In collaboration with Abhijith Prakash and Joerg Appenzeller at Purdue University

Metrology Opportunities?

- Develop protocol for 2D materials doping, characterization (physical and electrical)

- Establish correlations with electronic/photonic device response

- Materials Challenges
- Methods
- TMDs
  - Etching
- Summary

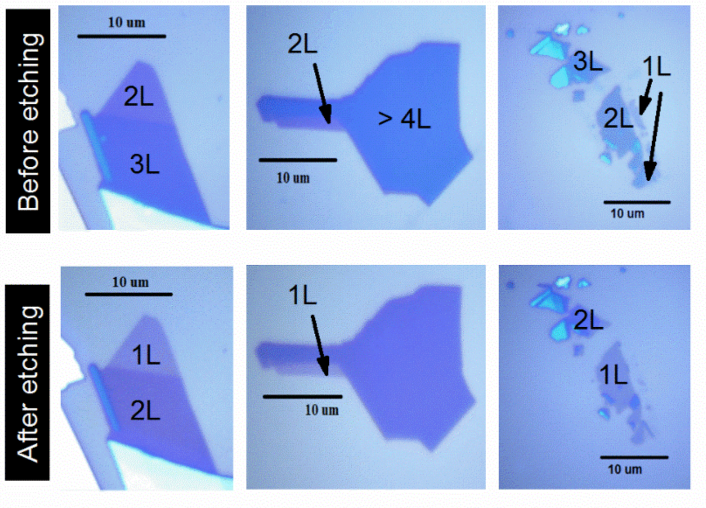

Atomic Layer Etching of MoS_2 crystal surface

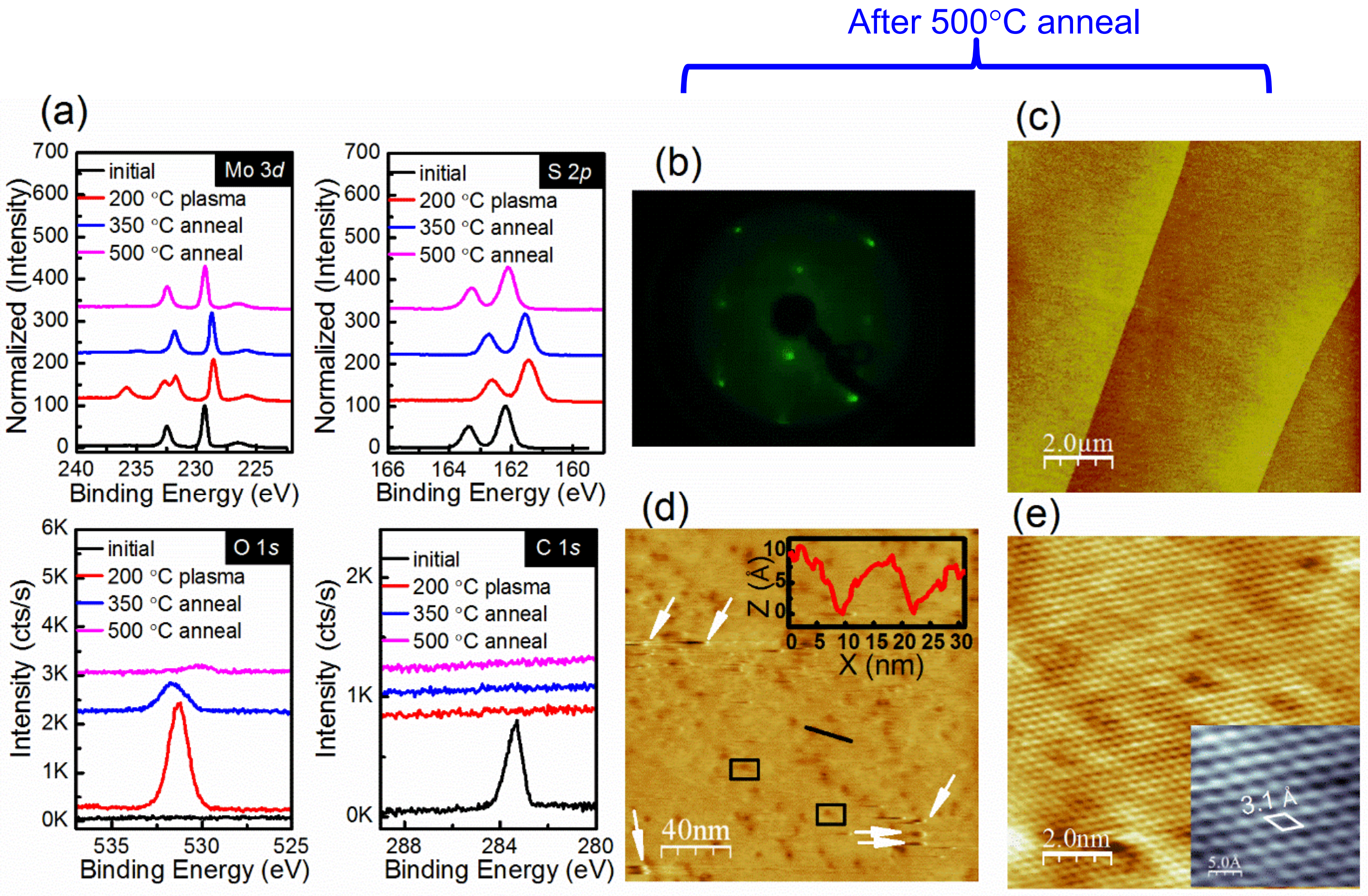

- Controlled oxidation of MoS_2 surface with a remote O_2 plasma
- Subsequently anneal O/MoS_2 to 500°C
- Removes layer of MoS_2 without underlying crystal disruption

ACS Applied Materials and Interfaces, **8** (29), 19119 (2016)

UT DALLAS

Atomic Layer Etching of MoS_2 flakes

- Controlled oxidation of MoS_2 surface with a remote O_2 plasma
- Subsequently anneal O/MoS_2 to 500°C
- Removes layer of MoS_2 without underlying crystal disruption

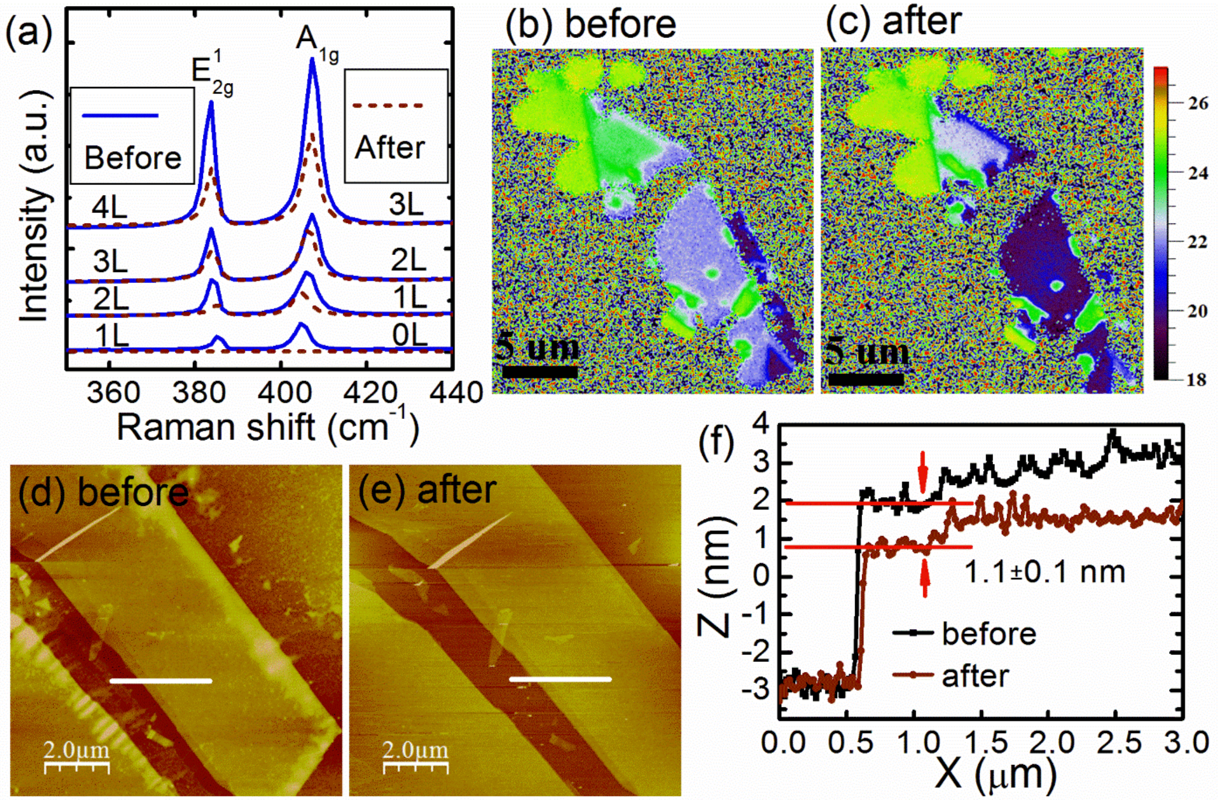

ACS Applied Materials and Interfaces, **8** (29), 19119 (2016)

Metrology Opportunities?

- Develop protocol for 2D materials etch rate measurements, characterization (physical and electrical)
- Establish correlations with electronic/photonic device response

- Materials Challenges
- Methods
- TMDs
    - New Phases
- Summary

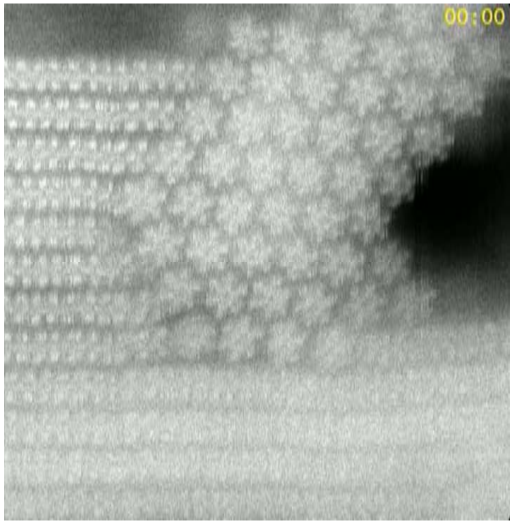

To end

Exfoliated $MoTe_2$: Rich in Surface Structures

Surface imperfections characterization of exfoliated CVT $MoTe_2$ crystals with STM, STS and STEM

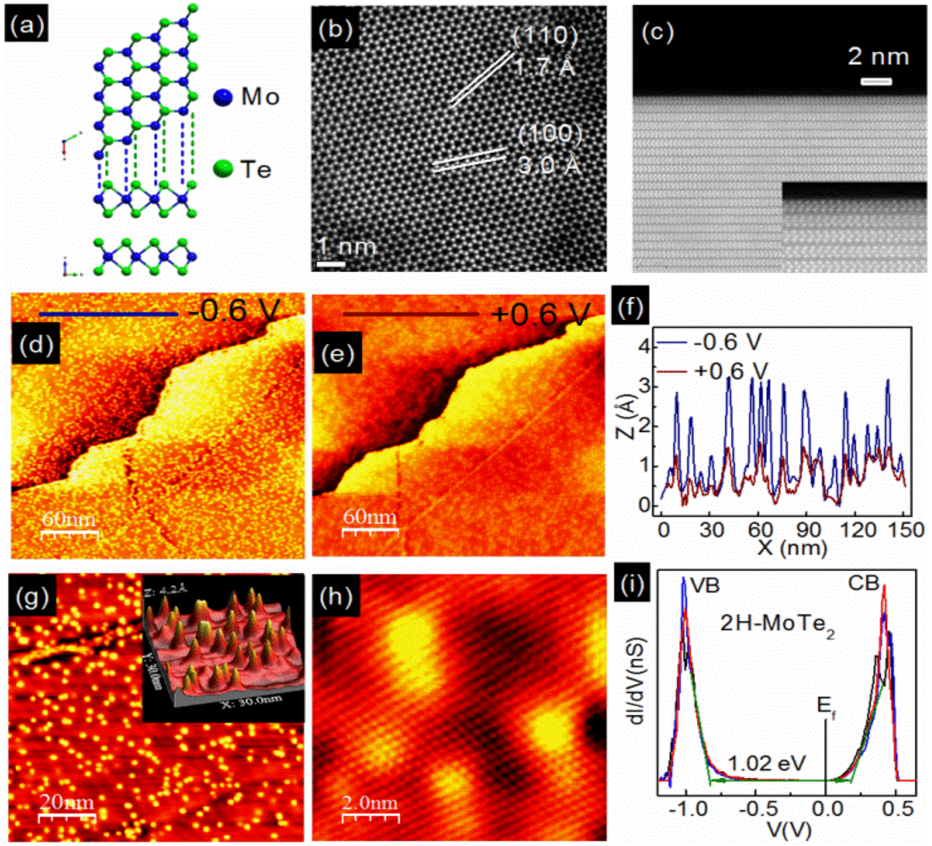

(a) Atomic structure of 2H-$MoTe_2$. (b) plan-view and (c) cross-section view [11-20] of high resolution STEM images with HAADF Z-contrast mode.

(d, e) Large-scale STM images (300×300 nm^2) of the same $MoTe_2$ surface region taken at a sample bias of -0.6 and +0.6 V, respectively, with a tunneling current of 0.6 nA. The step-edge in the figures is ~ 7 Å, corresponding to one layer of $MoTe_2$. (f) Line profiles crossing over the same region in d and e.

(g) A STM topographic image (100× 100 nm^2) shows the uniform circular shape of bumps/protrusions (bright spots). A 3D zoom-in image is shown in the inset of (g), indicate the average height of protrusions is 3±0.5 Å depending on sample biases and tunneling current. (h) High-resolution STM image of the represented 2H-$MoTe_2$ lattice decorated with protrusions. The image (g, h) are taken with V_b = -0.6 V, 0.4 V, respectively, and I_t = 1.5 nA. (i) STS measurements from multiple surface regions.

- 2H, 1T’ and T_d phases typically noted in the literature
- Variations in electronic nature of the surface
- Sensitivity of TEM vs. STM to defects

Advanced Materials 1606264 (2017)

MoTe$_2$: Beyond expected phases

Annealing MoTe$_2$ results in Te loss → phase changes → **Nanowire** formation

STM Image of annealed surface

XPS Spectra of annealed surface

STS of 2H and annealed surface

Electronic structure of (D) isolated and (E) NW bundle

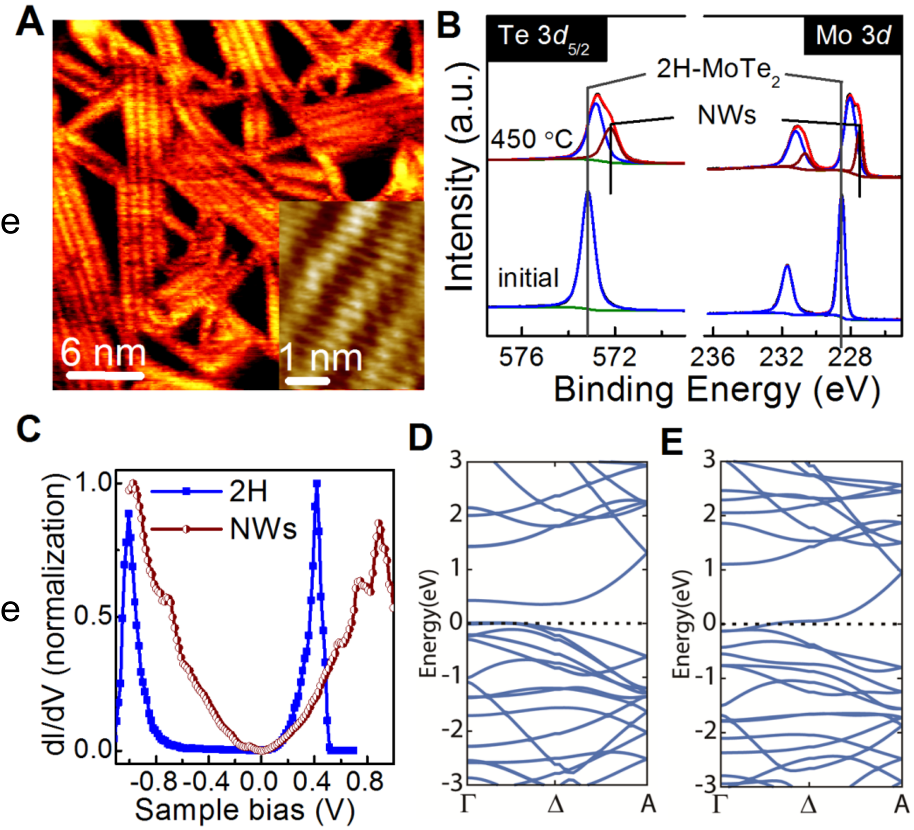

Advanced Materials 1606264 (2017)

MoTe$_2$: Beyond expected phases

- Te/Mo ratio on the initial surface is around 2.12±0.02, indicating a homogeneous Te rich environment.
- Subsequent thermal treatment reveals that the Te/Mo ratio is extremely temperature sensitive.

XPS spectra of the Te 3$d_{5/2}$ and Mo 3*d* core levels.

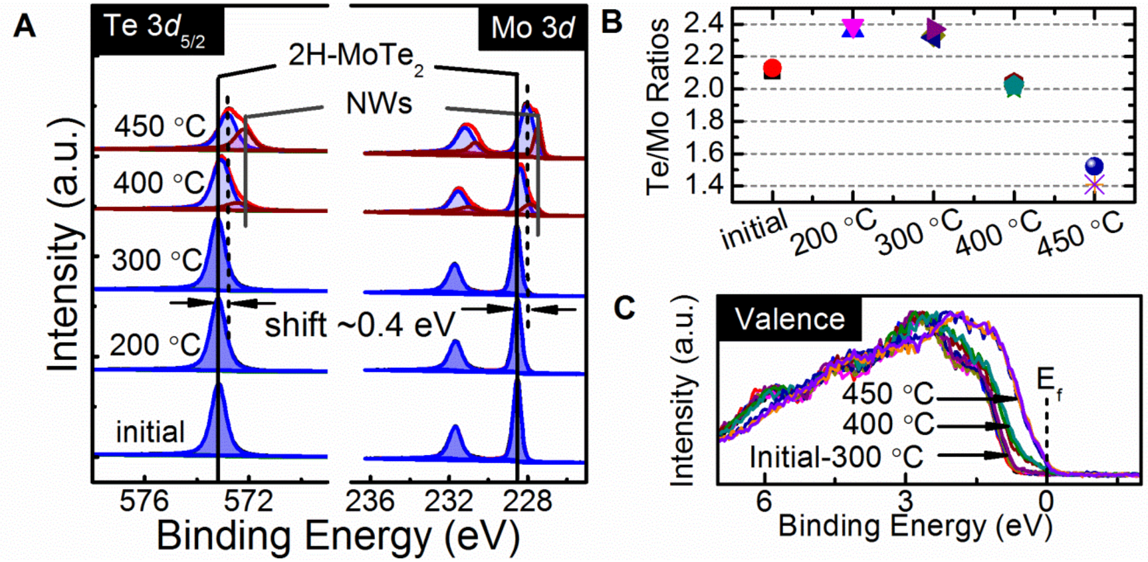

Derived Te/Mo ratios from the Te 3$d_{5/2}$ and Mo 3*d* spectra and measured on multiple surface regions.

Valence band regions measured on multiple surface regions.

Advanced Materials 1606264 (2017)

$MoTe_2$: Beyond expected phases

Schematic of the transition from 2H-$MoTe_2$ to Mo_6Te_6 NWs.

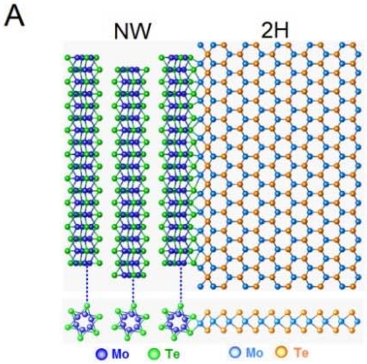

Plan-view image of Mo_6Te_6 NW bundles grown on 2H-$MoTe_2$ (0001) surface

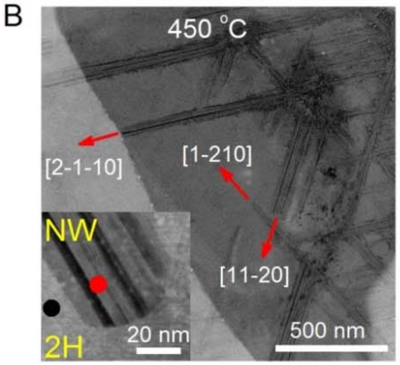

EDS analysis on top of Mo_6Te_6 NW bundles (red dot) and the nearby 2H-$MoTe_2$ region (black dot in the inset panel of B)

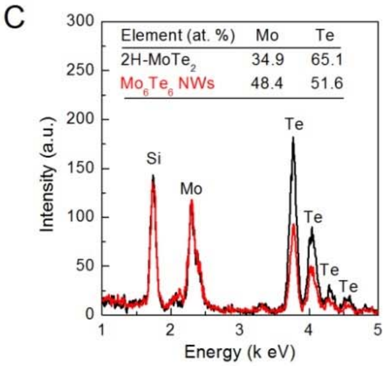

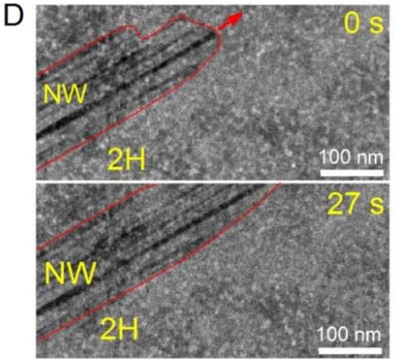

Time sequence images of 2H-$MoTe_2$ (0001) show a fast growth of Mo_6Te_6 NWs along the 2H-$MoTe_2$ <11-20> directions

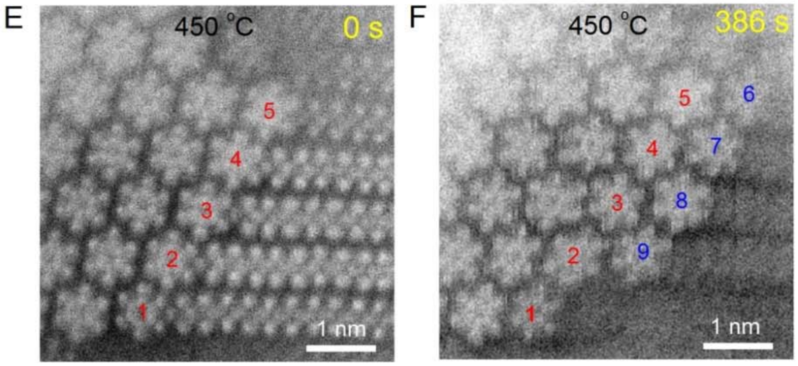

Time sequence images viewed along the 2H-$MoTe_2$ [11-20] direction (or Mo_6Te_6 [001])

© 2016 R.M.Wallace

Advanced Materials 1606264 (2017)

Metrology Opportunities?

- Develop database for 2D materials phases, characterization (physical and electrical)
- Establish correlations with electronic/photonic device response

- Materials Challenges
- Tools and Methods
- TMDs
- Summary

IEEE Spectrum

2D TMD Materials Challenges and Opportunities

- 2D TMD Materials may offer the ultimate scaling: a monolayer transistor channel
- Steep slope TFETs with useful “on” currents are under research now
- Cleaning process residues essential for reproducible properties
- Functionalization without substrate disruption possible, enables efficient ALD
- Surfaces can be far from perfect: defect density can be significant (several %)
- Contacts can be dominated by defects and reactions – deposition ambient details are important in interpretation of contact behavior
- Super acid wet passivation demonstrated on TM-sulfides, but not on selenides
- Substitutional *chalcogen* doping is possible
- Atomic layer etching routes are possible
- Impurities on geological and synthetic crystal surfaces can be substantial, progress has been made recently
- Large area, high quality (low defect/impurity) films needed for device progress

There appear to be MANY opportunities to establish metrology protocols, benchmarks and standards for the device community

Thin Solid Films **616**, 482 (2016)

Summary

- Relative to Si, TMDs exhibit relatively high intrinsic and extrinsic defects/impurities
    - Geological TMDs are far more inferior at this time.
    - Improvements in growth methods and purity have been noted
- Defects and interfacial chemistry, within the detection limit of in-situ surface analysis techniques, provide useful information to guide process development, tool/material requirements
    - Correlation to device behavior is possible and useful!
    - Opportunity to establish what constraints must be addressed
    - Details of process ambient are important!
- All researchers must be cognizant of the their materials properties when drawing conclusions
    - Physical characterization has limited sensitivity
    - Electrical characterization is very sensitive, but interpretation can be ambiguous

Thanks!

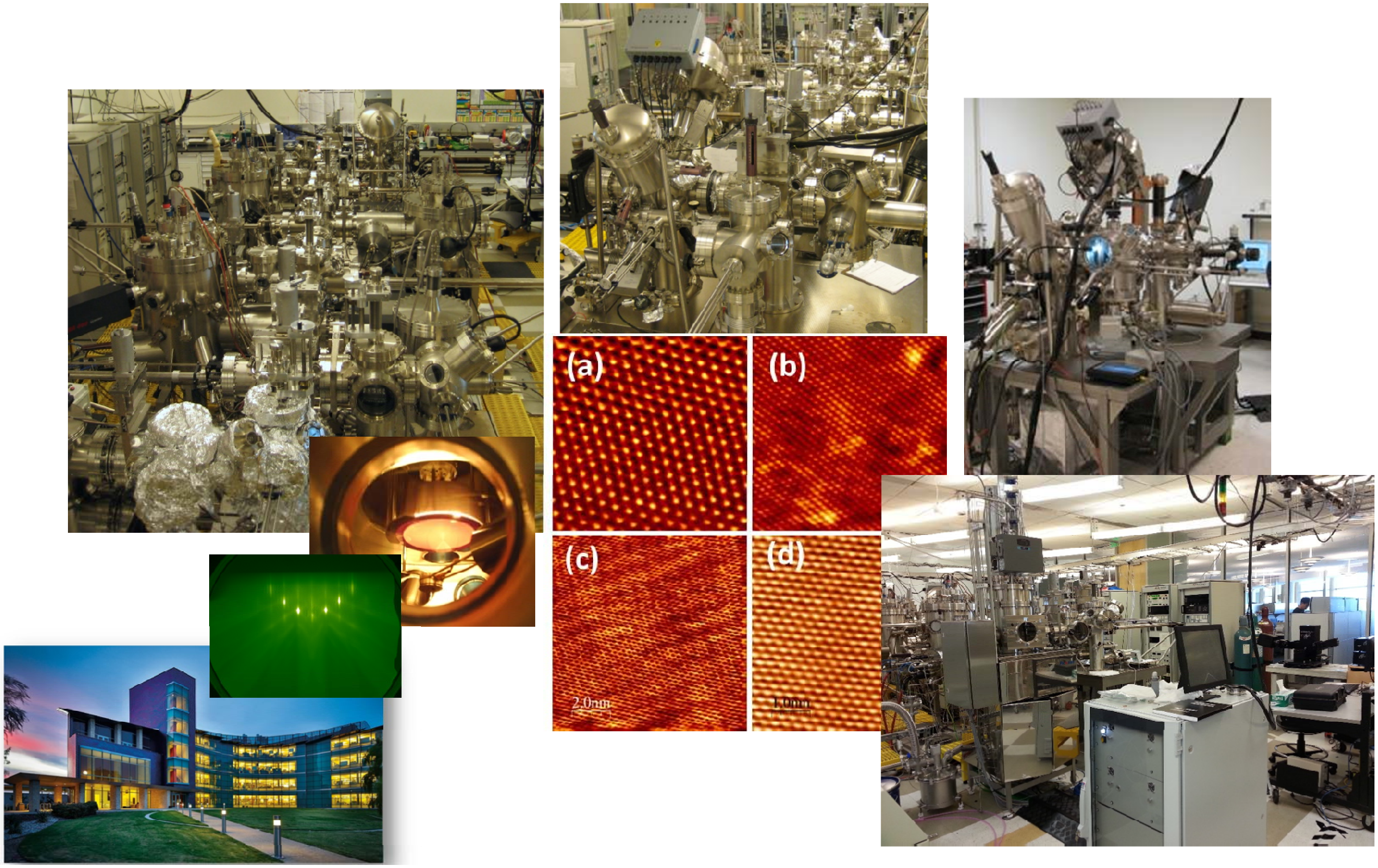

rmwallace@utdallas.edu

https://sites.google.com/site/robertmwallace01/